Int J Earth Sci (Geol Rundsch) (2018) 107:1321–1342
DOI 10.1007/s00531-017-1535-0

ORIGINAL PAPER

Geochemical study of travertines along middle-lower Tiber valley (central Italy): genesis, palaeo-environmental and tectonic implications

Francesca Giustini[1] · **Mauro Brilli**[1] · **Marco Mancini**[1]

Received: 18 July 2016 / Accepted: 30 August 2017 / Published online: 7 September 2017

Abstract Several travertine deposits dating to the Pleistocene outcrop along the Tiber valley between Orte and Rome. Mineralogically, they are mainly composed of calcite; various lithofacies (stromatolitic, phytoclastic, and massive) were identified and relatively wide ranges of carbon ($\delta^{13}C$ −8.11 to +11.42‰ vs. VPDB) and oxygen ($\delta^{18}O$ +22.74 to +27.71‰ vs. VSMOW) isotope compositions were measured. The isotope and chemical compositions of water and free gases, in some cases associated with the travertines, were also measured. Carbon isotope data show that several samples fall in the typical range of thermogenic travertine, i.e., linked to the addition of deep inorganic CO_2. The oxygen isotope composition of the springs associated with the travertine deposits points to travertine precipitation by slightly thermal water of meteoric origin. In general, these travertines are in association with, or close to, mineralised groundwaters (with slightly acidic pH, low thermalism, and enrichment in sulphates or sodium chloride) and rich CO_2 gas emissions, the origin of which may be linked to decarbonation reactions. The travertine bodies are locally connected with crustal structural lineaments favouring the circulation of ascending deep CO_2-rich fluids. Conversely, some samples show isotopic connotations of meteogenic deposits, representing travertines formed mainly from soil biogenic or atmospheric carbon dioxide generally present in shallow groundwater or surface water. According to their morphology and isotope data, these travertines may be attributed to the sedimentary environment of waterfalls. These new geochemical and morphological data are integrated with those already available in the literature regarding the study area and contribute to shedding light on palaeo-environmental conditions in western-central Italy during the Quaternary.

Keywords Travertine · Stable isotopes · Sources of CO_2 · Palaeo-temperature · Tiber valley · Italy

Introduction

Active and fossil travertine deposits are widespread in central Italy (Panichi and Tongiorgi 1976; Minissale 2004): the formation of most of them was due to the massive CO_2 emissions which mainly occurred on the Tyrrhenian side of the region. The origin of this CO_2 has long been debated, although there is now a general consensus in favour of viewing it as the result of a mixture of mantle-degassing and limestone decarbonation (Minissale 2004; Chiodini et al. 2004). The study of such travertine deposits, being associated with CO_2 emission, can thus contribute to the debate on the origin of CO_2 in central Italy, as they potentially represent a valuable archive of several sources of CO_2 in places where gas emanations are no longer visible (Gibert et al. 2009). According to the origin of CO_2, Pentecost (2005) separated continental carbonate deposits into *meteogene* and *thermogene* travertines. In the former, CO_2 originates in the soil at low temperature and, being derived from the atmosphere and 'soil respiration', may ultimately be considered meteoric in origin. Although such deposits generally form in cold spring waters, they are occasionally found where water, circulating deep beneath the surface, is heated and rises to the surface as hot springs, containing negligible thermally generated CO_2 (e.g., Bormio, Italy; Pentecost 1995). Travertines, in which the carbon dioxide is derived mainly

✉ Francesca Giustini
francesca.giustini@igag.cnr.it

[1] Istituto di Geologia Ambientale e Geoingegneria, CNR, Area della Ricerca di Roma1, Via Salaria Km 29,300, Monterotondo Stazione, 00015 Rome, Italy

from hydrolysis, decarbonation, or magmatic degassing, are defined as thermogenic; the waters responsible for these deposits are frequently, but not necessarily, hot and rich in dissolved salts. This classification is useful to this study, because it is based on the origin of CO_2 and can easily be adopted using the carbon isotope composition, since thermogene and meteogene travertines are, respectively, enriched or depleted in ^{13}C.

An alternative and widely used classification is based on an integrated approach, which involves the genetic environment and the presence of biota (Özkul et al. 2013; Capezzuoli et al. 2014; Gandin and Capezzuoli 2014). It comprises two main general classes of sub-aerial continental carbonate deposits: travertine and tufa. The former is generally hard and crystalline and related to abiotic processes in waters, typically hydrothermal in origin (Ford and Pedley 1996; Pedley 2009); they correspond more or less to the thermogene travertines defined by Pentecost (2005). 'Tufa' is more porous than travertine, and is rich in microphytes, macrophytes, and invertebrate and bacterial remains (Ford and Pedley 1996); it generally formed in waters of ambient temperature and may correspond to meteogene deposits. When this classification is applied, some uncertainties may occur regarding the interpretation of the deposits in cooled thermal waters, where tufa-like deposits may be precipitated when the water temperature decreases with distance from the spring source; the term 'travitufa' has been suggested for these types of travertine (Capezzuoli et al. 2014). In the present study, as we are mainly interested in the origin of carbon dioxide and in the distinction between deep and surface circulating fluids, it is convenient to discuss any carbonate deposits in terms of their thermogenic or meteogenic nature. In addition, this nomenclature allows us to describe and discuss these deposits without any preconceived ideas about precipitation conditions, such as water temperature (Claes et al. 2015).

The carbon and oxygen isotope compositions of travertines provide useful information which may reveal both the source of the CO_2 and precipitation conditions (e.g., temperature and isotope composition of precipitation water) (Friedman 1970; Panichi and Tongiorgi 1976; Gonfiantini et al. 1968). Panichi and Tongiorgi (1976) derived an empirical linear equation linking the carbon isotopic composition of CO_2 and travertine carbonate, and this approach was later applied elsewhere to calculate the isotopic composition of the parental CO_2 of a travertine and to identify the carbon source (Minissale et al. 2002; Minissale 2004; Piccardi et al. 2008; Kele et al. 2008, 2011; Sierralta et al. 2010; Rodríguez-Berriguete et al. 2012; De Filippis et al. 2012). In contrast, data on travertine oxygen isotopes have mainly been used in palaeohydrological and palaeoclimatological research (Pazdur et al. 2002; Minissale et al. 2002; Andrews 2006).

Several travertine deposits outcrop along the Tiber valley, representing an ideal archive for stratigraphic and geochemical studies. The valley is a morpho-tectonic depression of extensional origin, filled with syn-extensional sedimentary and volcanic successions of Pliocene–Quaternary age up to 1 km thick (Funiciello and Parotto 1978; Barberi et al. 1994; Cavinato et al. 1994; Mancini and Cavinato 2005; Funiciello and Giordano 2008). Earlier isotopic studies on these travertines date back to the 1970s (Manfra et al. 1976; Barbieri et al. 1979). More recently, Minissale et al. (2002) recognised in the Tiber valley the dividing line between a western sector, where deposits exhibit characteristics typical of a thermogenic (thermal spring) origin, and an eastern sector, in which they show meteogenic (low-temperature) characteristics. In their hydraulic reconstruction, the above authors also found that the travertine-precipitating waters east of the Tiber valley have shallower flow paths than those to the west (Minissale et al. 2002).

In this study, we present a morphological characterisation and describe the mineralogical and isotopic features of several Quaternary travertine deposits of the Tiber valley, in the section between Orte and Rome (Fig. 1). The isotope and chemical compositions of water and free gases, in some cases associated with both fossil and active depositing travertines, were also studied. The aim of this research was to shed light on the palaeo-environmental and geological conditions that allowed such extensive travertine deposition in this context during the Quaternary. The relationship between travertine deposits, tectonics, the volcanic activity of the Tyrrhenian sector, and climatic forcing are discussed, considering circulation and interaction between surface and deep waters and the carbon sources which contributed to the formation of travertine.

Geological and hydrogeological setting

The study area (Fig. 1) corresponds to the middle and lower valley of the Tiber river between Orte and Rome, west of the central Apennines (central Italy), the structural setting of which results from the onset and eastward migration of an SW–NE directed extension related to the opening of the Tyrrhenian Sea back-arc basin (Patacca et al. 1990; Cavinato and De Celles 1999; Carminati and Doglioni 2012). The middle and lower stretches of the Tiber valley do in fact correspond to two adjoining NNW–SSE-directed, morpho-tectonic depressions of extensional origin: the Paglia-Tevere Graben and the Rome Basin, filled by syn-extensional sedimentary and volcanic successions of Pliocene–Quaternary age up to 1 km thick, at present crossed axially by the Tiber (Funiciello and Parotto 1978; Barberi et al. 1994; Cavinato et al. 1994; Mancini et al. 2004; Mancini and Cavinato 2005;

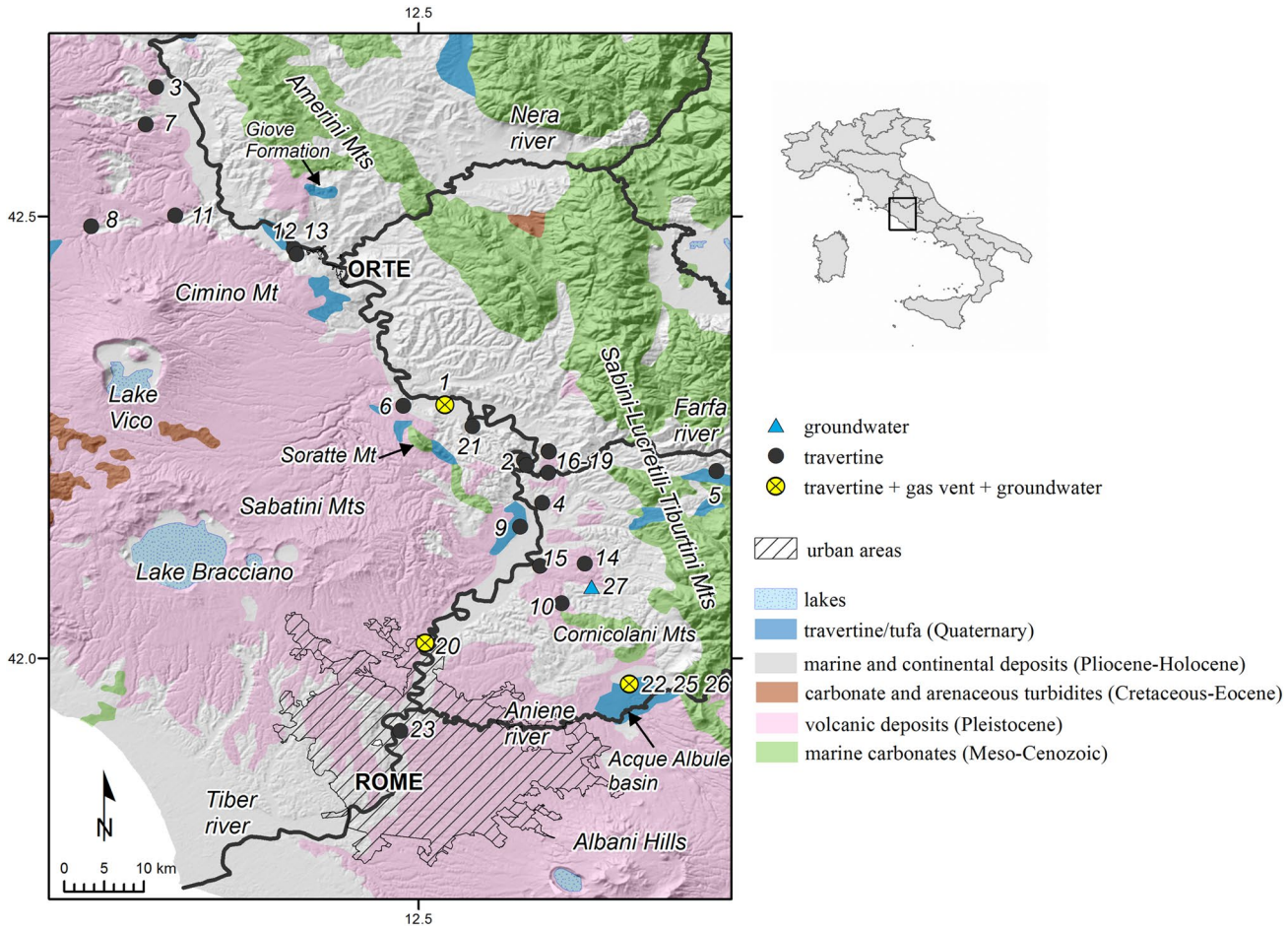

Fig. 1 Geological map of the Tiber valley (from SGI-ISPRA geoportal available at http://sgi.isprambiente.it/geoportal/catalog/main/home.page) showing location of travertine sites and sampling points (travertines, waters, and gas emissions)

Funiciello and Giordano 2008). These successions overlie with angular unconformity Meso-Cenozoic (Trias-late Miocene) pelagic carbonate and siliciclastic successions, piled into thrust sheets during the Tortonian–Messinian (Cavinato and De Celles 1999; Cosentino et al. 2010; Mattei et al. 2010). The basins are bounded to the east by the ridge of the Amerini–Sabini–Lucretili–Tiburtini Mountains, where the carbonate and siliciclastic substrate are exposed, and to the west and south by the Quaternary volcanic complexes of the Sabatini Mountains and the Alban Hills; the basins are also separated longitudinally by the alignment of the Soratte and Cornicolani Mountains, a 30-km-long carbonate ridge partly buried by the Plio-Quaternary cover. The structural style has thus been dominated since the late Zanclean by grabens and horsts bounded by major NNW–SSE-trending normal faults (the 'Apennine' trend), and longitudinally cut by minor NE–SW-running normal and transtensional faults (Funiciello and Parotto 1978; Faccenna and Funiciello 1993). Minor N–S-trending, right-lateral slip faults, and NNW–SSE-trending oblique normal faults have been identified in the areas of Mt. Soratte-Fiano and the Cornicolani Mts. (Faccenna 1994; De Rita et al. 1995).

The infill of the Paglia–Tevere and Rome basins is characterised by prevalent offshore marine and transitional (fluvio-deltaic) terrigenous deposits which filled the subsiding basins during the Zanclean–Calabrian interval, but which have been replaced since the late Early Pleistocene (1.4–1.0 Ma) by syn-uplift continental sediments and distal sub-aerial volcanic products from the Roman Magmatic Province (Mancini et al. 2004; Mancini and Cavinato 2005). The magmatic activity along the western margin of central Italy, the consequence of crustal thinning due to the extension of the Tyrrhenian area, generated the large stratovolcanoes and volcanic complexes of Vulsini (0.6–0.15 Ma), Vico-Cimino (0.4–0.1 Ma), Sabatini (0.6–0.04 Ma), and the Alban Hills (0.6–0.02 Ma), with the eruption of large volumes of potassic and ultrapotassic lavas and pyroclastics (De Rita et al. 1993; Barberi et al. 1994; Funiciello et al. 1994; Karner et al. 2001; Sottili et al. 2004; Peccerillo 2003;

Funiciello and Giordano 2008; Marra et al. 2009). Intra-Apennine volcanism also occurred in the same period, and consists of some monogenic pyroclastic centres and lava flows, e.g., San Venanzo (0.3 Ma), Cupaello (0.6–0.3 Ma), and Polino (0.3 Ma), characterised by ultrapotassic melilititic (kamafugites) composition (Peccerillo 2003). Travertines are found at the top of, or interbedded with, fluvial deposits and pyroclastics (Figs. 2, 3).

The structural and stratigraphic complexity of the whole study area controls its hydrogeological setting, with complexes consisting of clastic heterogeneous marine to transitional deposits or alluvial deposits (Boni et al. 1988). The first complex is defined as poorly cemented sandstone and mud interbedded with gravels, conglomerates, and distal pyroclastics; the second consists of recent alluvial deposits (10–20 m thick for the tributaries and more than 60 m for the main Tiber valley; Mazza and La Vigna 2011) which hosts shallow groundwater circulation. An underlying carbonate unit of the Meso-Cenozoic substrate constitutes the main regional aquifer. Travertine deposits make up local hydrogeological complexes, with medium–high permeability due to porosity in phytoclastic/waterfall facies and local fracturing or karstification in massive travertine facies. Several thermal and cold mineral springs are scattered across the valley and along the boundaries of the limestone and volcanic formations (Capelli et al. 2012). The cold springs are generally composed of Ca(Mg)–HCO_3. The thermal or warm waters ($T > 15$ °C) commonly show compositions between Ca(Mg)–HCO_3 and Ca–SO_4 (the latter component deriving from the dissolution of the Triassic anhydrite layers at the base of the Mesozoic carbonate bedrock) or between Ca(Mg)–HCO_3 and Na–Cl (probably due to the dissolution of Miocene–Pliocene marine evaporites embedded in the shallower parts of the flow path) (Minissale et al. 2002; Minissale 2004). Currently, only a few springs precipitate travertine in central Italy (e.g., Tivoli, Viterbo, Saturnia; Minissale 2004): they are characterised by CO_2-rich gas emissions, temperatures higher than 20 °C (up to 65 °C at Viterbo spring), and Ca–HCO_3 composition.

Tiber valley travertines

There are many travertine outcrops in the middle and lower Tiber valley (Figs. 2, 3), the detailed lithochronostratigraphy of which is shown in the recent geological maps of the Paglia–Tevere and Rome basins (Mancini et al. 2004; Funiciello and Giordano 2008).

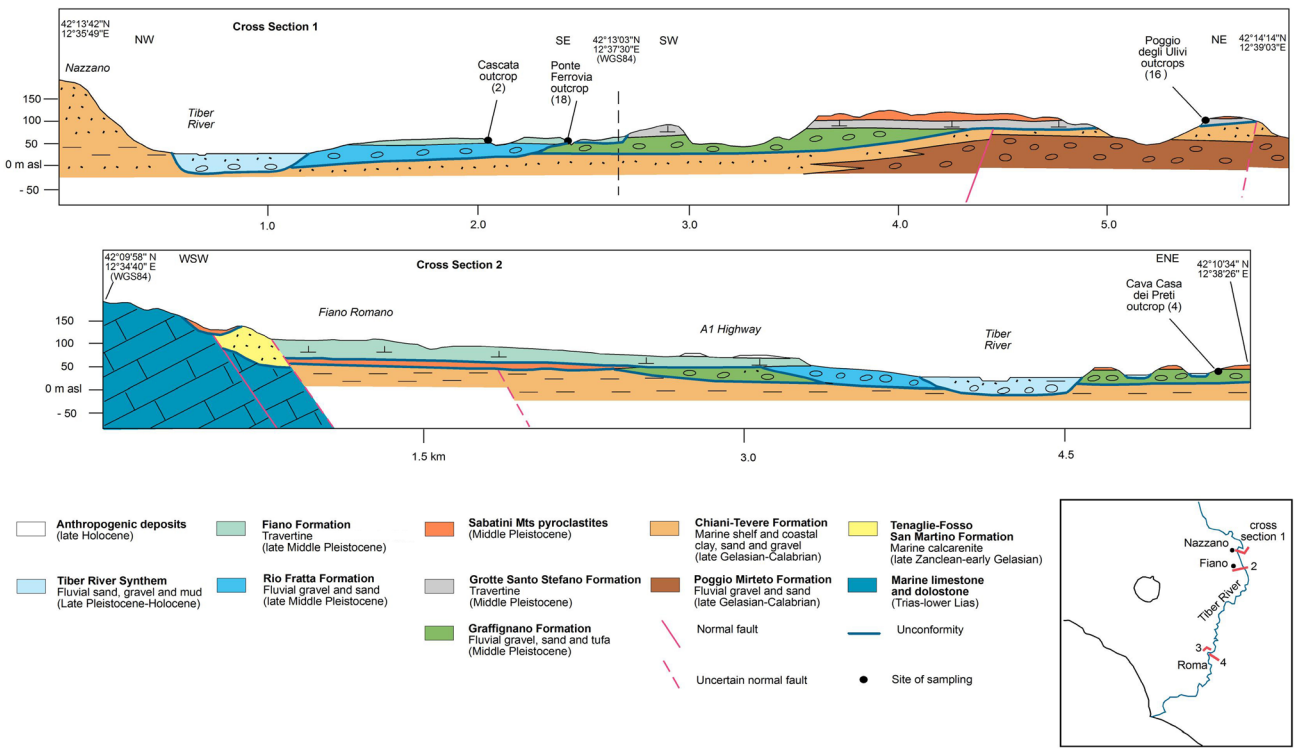

Fig. 2 Geological cross sections showing the stratigraphic architecture of the middle Tiber valley, based on the geological map of Mancini et al. (2004). Cross sections highlight stratigraphic relations among travertine units and fluvial siliciclastic deposits and pyroclastics. It should be noted that the cross sections intercept some of the sites of sampling. Sampling site number in *brackets*

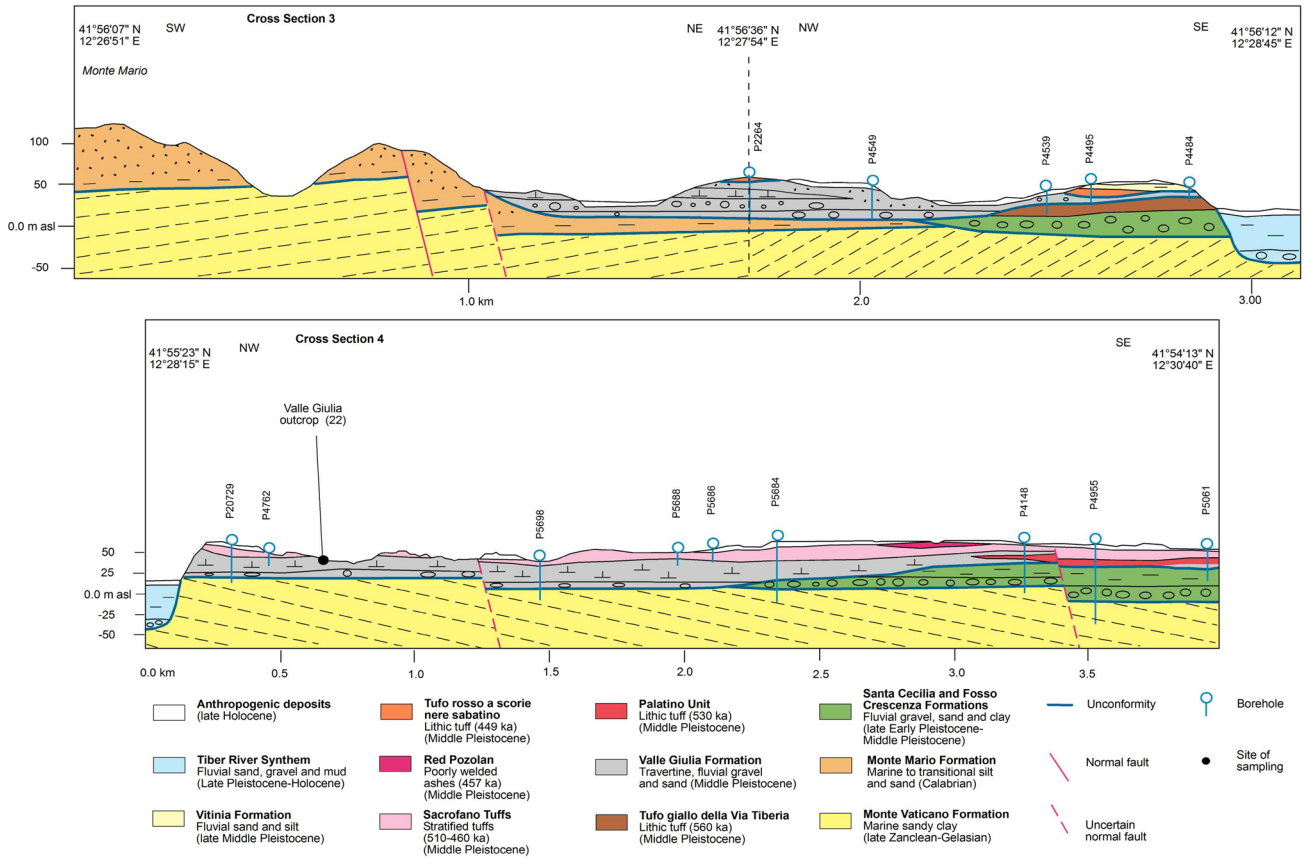

Fig. 3 Geological cross sections of the lower Tiber valley in the centre of Rome, based on the geological map of Funiciello and Giordano (2008) and borehole data from Ventriglia (2002). Geographical location of the cross sections is shown in Fig. 2. Sampling site number in *brackets*

Middle Tiber valley

In the middle valley (Paglia–Tevere Graben), the oldest travertine units of Emilian age (approximately 1.4–1.2 Ma) are: (1) the travertine deposits of the Giove Formation (Mancini et al. 2007), which are up to 40-m thick, regressive on coastal marine sands, and outcrop at the south-western margin of the Amerini Mountains (Fig. 1); (2) travertines overlying the 1.3Ma ignimbrite produced by Cimino Mt. stratovolcano activity (Mancini et al. 2004). Both these units are fluvio-lacustrine in origin and are mostly composed of phytoclastic travertines with prevailing mudstone and wackestone.

Middle Pleistocene travertine deposits are more widespread in the Paglia–Tevere graben and are represented by two main lithostratigraphic units, the Grotte Santo Stefano Formation and the Fiano Formation, lying on the fluvial terrigenous terraces (Fig. 2), and by minor carbonate deposits interlayered within the alluvial formations (Mancini et al. 2004).

The Grotte Santo Stefano Formation outcrops near structural alignments, and is dated to 350–250 ka on the basis of its stratigraphic correlation with encasing pyroclastics (Mancini et al. 2004). It is mostly composed of phytoclastic and phytohermal travertines referable to the fluvial barrage depositional model proposed by Pedley (2009), e.g., at the 'Poggio degli Ulivi' site (Colle Verrucola) (Fig. 2). Older freshwater travertines (about 500–450 ka) are found on the topmost strata of the fluvial Graffignano Formation, and are referred to as fluvio-palustrine facies. This lithostratigraphic unit was sampled at the 'Cava dei Preti' (Fig. 2) and 'Ponzano' sites, which are characterised by cemented sands with calcified nodules and tubules, and at the 'Ponte Sfondato' site, which represents a floodplain environment typified by slightly cemented calcareous sand.

The Fiano Formation outcrops at: (1) the 'Fiano Romano' site (Fig. 2), where it is composed of 40-m-thick phytoclastic and hydrothermal travertines gently wedging out eastward; and (2) the Farfa-Tevere confluence, where encrusted bioherm travertines related to a waterfall environment ('cascade model' of Pedley 1990) overlie fluvial sands and gravels (e.g., at the 'Cascata' and 'Ponte Ferrovia' sites; Figs. 2, 5d). At the latter site, stromatolitic and phytoclastic facies both occur (Fig. 5a), with well-stratified stromatolitic travertines

around 1 m in thickness characterising the summit of the outcrop (Fig. 5b); travertine presenting phytoclastic facies, in which the phytoclasts were deposited either in situ or after limited transport, is recorded in the lower middle part of the deposit. These structures exhibit a certain degree of orientation due to water flow (Fig. 5c). Some examples of travertine tubes are visible (Fig. 5d), consisting of protuberant cylinders of travertine forming natural spouts at the top of small waterfalls, and considered a sub-type of prograding cascades (Pentecost 2005). The association of these features can be attributed to the sedimentary environment of a waterfall. Oncolitic facies have also been identified, next to biohermal facies, suggesting moderately flowing water in a fluvial setting.

Smaller deposits are found buried under the Holocene alluvial plain, as at the 'Piana Bella' site, where a massive travertine (i.e., mudstone and wackestone, with a matrix-supported texture; Fig. 4d) has been identified, or the 'Acqua Forte' site, where phytoclastic travertines are actively depositing at the emergence of the spring, from mineralised-CO_2 degassing water.

Lower Tiber valley

Two well-defined depositional settings are known within the Rome Basin, one at Tivoli, due to tectonic basin infill (Faccenna et al. 1994, 2008) and the other in Rome, where travertines are interbedded with fluvial deposits and pyroclastics.

Near Tivoli, a town about 25 km east of Rome, near the Alban Hills volcano, is one of the largest Italian travertine deposits: the *Lapis Tiburtinus*, i.e., the stone of *Tibur*, the former name of Tivoli, from which the term travertine was derived in medieval times. Here, a remarkably thick (up to 90 m) plateau of compact, massive lacustrine, and hydrothermal travertines record the complex polycyclic infilling of the Acque Albule basin within the latest Middle Pleistocene–Holocene interval (Faccenna et al. 1994, 2008).

In Rome, continental carbonates are mainly due to the infilling of a multiple stack of fluvial-incised valleys, interbedded with well-dated pyroclastic units along the valleys of the Tiber and Aniene rivers. The oldest travertine deposits in Rome are known as the Santa Cecilia Formation, correlated with Marine Isotope Stages 16–15 (Funiciello and Giordano 2008; Marra and Florindo 2014), and are mostly found in subsoil. The prominent Valle Giulia Formation outcrops in the northern-central part of Rome (Fig. 3): it is correlated with Marine Isotope Stages 14–13 (about 550–500 ka), is mainly composed of phytoclastic and phytohermal travertines typical of a fluvial environment, and features large-scale cross bedding. Although travertine samples from the 'Valle Giulia' site are similarly characterised by the presence of plant fragments, they are also laminated and yellow-brownish in colour, sometimes with semi-translucent calcite veins (Fig. 4e, f). Minor travertine deposits, such as those at the 'Prima Porta' site, with a massive, compact aspect, are found interbedded within the late Pleistocene–Holocene alluvium.

Travertines and local structural setting

The travertines of the Middle and Lower Tiber valley are generally located along local tectonic structures. The oldest units of Early and Middle Pleistocene age (the Giove and Grotte Santo Stefano Formations) run along the main NNW–SSE-trending lineaments, such as the main boundary SW-dipping normal faults of the Amerini Mountains and the Soratte–Cornicolani ridge. They widen to the SW, dipping along the regional topographic slope and transversally to the axis of the Apennine Chain, and are interfingered with pyroclastic units.

The younger units of Middle–Late Pleistocene and Holocene age (~200 ka), such as the Fiano Formation and the Tivoli travertines, are related to N–S-trending dextral strike-slip faults and NNE–SSW-striking oblique faults cross-cutting the Mt. Soratte-Cornicolani horst and bounding the small tectonic depression of the Acque Albule Basin (Faccenna 1994; De Rita et al. 1995; Faccenna et al. 2010). The different geographical distribution of travertine deposits, from Early–Middle to Middle–Late Pleistocene, is thought to be related to a local change in the active tectonic regime in western-central Italy (at the periphery of the volcanic complexes) from a pure NE–SW-directed extension to a N–S-trending transtension. This change also controlled the last stages of volcanism and hydrothermal circulation (Faccenna et al. 2010).

Methods

The locations of travertine, water, and gas sampling are shown in Fig. 1, which includes both travertine samples reviewed from the literature and travertines, waters, and gases collected for this study and never examined previously.

The carbon ($\delta^{13}C$) and oxygen ($\delta^{18}O$) isotope ratios of travertine were measured from ~0.2 mg powder samples made with the modified phosphoric acid method of McCrea (1950). Isotope analysis was generally carried out on bulk carbonate; in sites 4 and 21, nodules and tubules were selected for analysis. A Finnigan Kiel II—Carbonate Device interfaced with a Finnigan MAT 252 mass spectrometer was used for analyses.

The samples were also analysed for their mineralogical composition on a Philips PW1840 diffractometer (CuKa/Ni: 40 KV and 20 mA). Semi-quantitative mineral composition was determined with XPowder12 free-ware software (available online at http://www.xpowder.com).

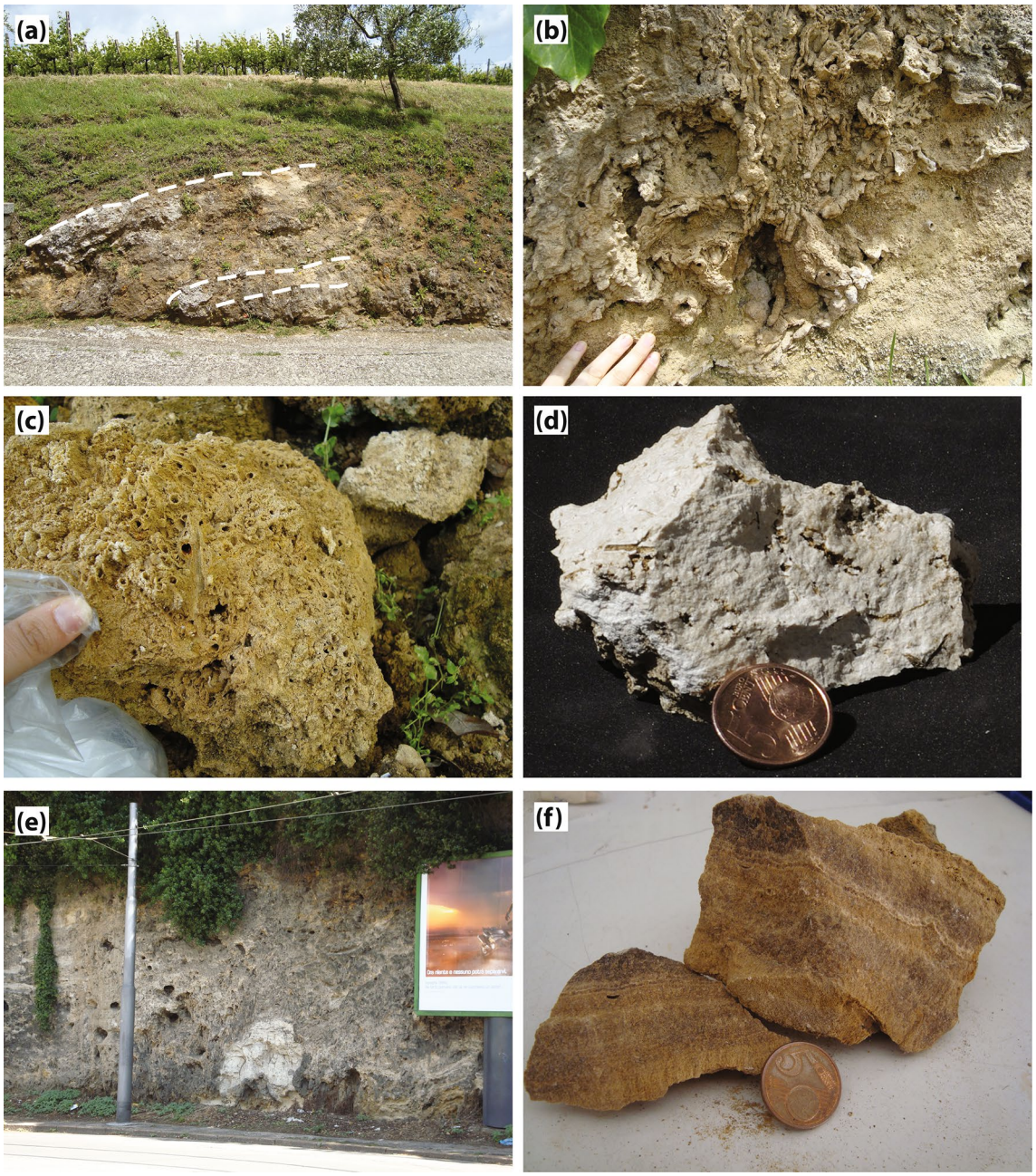

Fig. 4 Field and hand specimen images of travertines from Tiber valley. **a** Gentle slope of the travertine outcrop, that can be interpreted as a slope deposit, possibly laterally or vertically transitional with waterfall and pool association, of 'Poggio degli Ulivi' site; **b** phytoclastic travertine from 'Poggio degli Ulivi' site; **c** site 'Cascata', phytoclastic travertine formed by tubular, coarse fragments mostly of encrusted reeds; **d** hand specimen of massive travertine from 'Piana Bella' site; **e** travertine deposit of 'Valle Giulia'; **f** laminated travertines, with semi-translucent calcite veins, from 'Valle Giulia' site

Four locations were also characterised by a vigorous-free gas phase that was collected with the inverted bottle technique (Meents 1960) and stored in pre-evacuated 25-ml stainless steel canisters sealed with two vacuum stop-cocks. For rapid measurement of chemical composition, a Dräger X-am 7000 equipped with an IR sensor was used in the field. After off-line purification in a vacuum line, CO_2 was analysed for carbon isotope composition on a Finnigan MAT 252 mass spectrometer.

Chemical and isotopic analyses were also performed on five water samples, with temperature, pH, redox potential (Eh), and electrical conductivity (EC) measured in the field with a multi-parameter probe; alkalinity was measured by titration with 0.05 N HCl. In the laboratory, major anions (Cl

and SO_4) and cations (Ca, Mg, Na, and K) were determined by ion chromatography (Metrohm) on filtered and filtered/acidified samples, respectively; the analytical precision, as %RSD based on replicate analysis of standard solutions, was <5%. The $^{18}O/^{16}O$ isotopic ratios of water samples were determined with the equilibration technique (Epstein and Mayeda 1953).

The results of isotope analyses on travertine, water, and CO_2-free gas are reported in the usual delta (δ) notation, representing relative deviation in parts per mil (‰) with respect to the following international standards: VPDB for carbon isotopes and VSMOW for oxygen isotopes. Standardisation for calcite samples was conducted with laboratory standards calibrated against NBS-18 and NBS-19 standards, and water samples according to laboratory standards calibrated against SMOW, GISP, and SLAP. The internal standard precision of isotopic analysis for both $\delta^{13}C$ and $\delta^{18}O$ was ±0.1‰.

Results

Travertine facies

In the Tiber valley, where travertines are located at varying topographic heights (from about 20 up to 400 m a.s.l.) (Table 2), four main facies were identified: phytoclastic, stromatolitic, coated grains (as described by Pedley 1990; Pentecost 2005; Ozkul et al. 2014), and massive travertine when there were no particular structures to be identified on a macroscopic basis. The association of these facies, integrated with field observation of the morphology of the deposits, indicates their depositional environment (Table 1).

The phytoclastic facies consist of fragments of carbonate encrustations on vegetable supports (Fig. 4a–c), with a detrital texture. The fragments include leaf imprints, stems (sometimes branching), twigs, tree trunks, and cylindrical clasts, which were encrusted during and/or after transport to their depositional setting (Pedley 1990). The dimensions of the phytoclasts vary from tree trunks about 5 cm in diameter to small twigs and leaves of a few millimetres; in some cases, large cavities characterise tree-trunk moulds. Phytoclastic facies formed in palustrine-to-shallow lacustrine conditions as well as several fluvial settings. These deposits can also be found in shallow braided rivers with a barrage system produced by the destruction of bryophytes and macrophytes. This facies also occurs in waterfall environments. In some cases, calcified stems were found oriented in life position (phytohermal facies).

The stromatolitic facies are composed of several laminae, with thicknesses of up to 1 cm for each lamina, and a sub-horizontal to convex-up laminated texture (Fig. 5b). The depositional environment of these dense, laminated deposits is generally associated with a sedimentary environment of fast-flowing water, such as stepped cascades in a fluvial setting.

Oncoids are the main component of coated grains facies; they are small grains (from <1 to 5 mm in diameter), spherical or spheroidal in shape, the growth of which is actively triggered by microbial activity. This facies is characterised by a grain-supported texture with a certain amount of matrix in the 'Cascata' and 'Ponte Ferrovia' sites, whereas the coated grains in the 'Ponte Sfondato' site are matrix-supported. Oncoids are typical of rivers and sluggish flow regimes.

'Massive travertine' consists of a hard, quite dense crystalline material, which appears structureless or with horizontally bedded and inclined layers, a few centimetres to decimetres thick. It may occur as mudstone and wackestone, with a matrix-supported texture. This kind of material is associated with low-energy environments, such as pools, shallow lakes (e.g., the 'shallow lake-fill deposits' at Tivoli, in Chafetz and Folk 1984), or floodplains in fluvial systems.

Stable isotope geochemistry and mineralogy of travertines

Table 1 lists the carbon and oxygen isotope values for the analysed travertine samples. The mean isotope values (Table 2) are plotted in Fig. 6, in which the new data are integrated with those already available in the literature regarding the study area (Manfra et al. 1976; Minissale et al. 2002; De Filippis et al. 2013).

Isotopic values fall between −8.11 and +11.42‰ (average + 4.05‰) vs. VPDB for carbon and between +22.74 and +27.71‰ (average + 25.11‰) vs. VSMOW for oxygen. In Fig. 6, which reveals no evident correlation between $\delta^{13}C$ and $\delta^{18}O$ values, the Tiber valley travertines are grouped according to facies identified in the field or described in the literature. Samples of phytoclastic and stromatolitic facies, as well as calcified nodules and tubes, tend to group towards the most positive $\delta^{18}O$ values in the diagram, whereas the travertines with massive travertine facies are characterised by more negative $\delta^{18}O$ values. A large variation is shown by $\delta^{13}C$, which ranges between −8.11 and +11.42‰ VPDB, but no univocal relationship was found between the different facies and the carbon isotopes: although the massive travertine facies are characterised by positive values of $\delta^{13}C$ (from +3.52 to +11.42‰), the phytoclastic facies span the entire range of carbon isotope values. For comparison, Fig. 6 also displays the field encompassing most of the isotopic values for travertines from central-southern Italy reported in the literature (data after Gonfiantini et al. 1968; Panichi and Tongiorgi 1976; Buccino et al. 1978; Ferreri and Stanzione 1978; Carrara 1994; Minissale et al. 2002; Minissale 2004; Ascione et al. 2013; Raimondi et al. 2015; Vignaroli et al. 2016). It shows that the Tiber valley travertines mostly fall

Table 1 Overview of the Tiber valley travertine deposits examined for this study, with description of sites and samples. Stable isotope and mineralogical compositions based on XRD analyses are reported (*tr* trace amount)

ID	Site	Site description	Sample	Sample description	$\delta^{18}O$ ‰ VSMOW	$\delta^{13}C$ ‰ VPDB	Mineralogy
1	Acqua Forte Lat: 12.5303° Long: 42.2872°	Spring mound, with recent (i.e., actively forming) travertine, ~1 m high. Calcified twigs, leaves, and bushes in life position (phytohermal facies) were identified. Close to spring, an abandoned borehole was used to sample free gas phase and water	T1a	Phytohermal travertine from spring orifice	25.49	9.55	Calcite
			T1b	Phytohermal travertine, distal from the spring	26.39	11.66	
2	Cascata Lat: 12.6201° Long: 42.2230°	Terrace (~10 m high), gently inclined and about 3-ha wide. Crudely bedded phytoclastic travertine with coated grains and calcified plant remains, characteristic of this outcrop, interpreted as a waterfall travertine developing on a moderate-angle slope	T2a	Lamina of calcified plant remain	24.86	−1.22	Calcite
			T2b	Coated grains	24.58	−1.35	
			T2c	Lamina of calcified plant remain	24.59	−3.29	
			T2d	Lamina of calcified plant remain	24.71	−1.72	
4	Cava Casa dei Preti Lat: 12.6398° Long: 42.1752°	Quarry of fluvial gravel, ~25 m high. A 2–3-m tabular level rich in calcified tubules and nodules was sampled immediately above bottom of sequence	T4a	Tubule	24.41	−1.78	
			T4b	Nodule	24.33	−3.17	
9	Fiano Romano Lat: 12.5898° Long: 42.1423°	Tabular beds of massive travertine gently dipping along-slope towards Tiber plain, interpreted as deposited distally with respect to source area	T9a	Phytohermal	25.06	3.33	
			T9b	Massive, brownish	26.20	7.26	Calcite + Quartz (tr)
			T9c	Massive, brownish	26.55	8.43	
			T9d	Massive	24.35	7.18	
			T9e	Rafts	23.67	8.32	
15	Piana Bella Lat: 12.6358° Long: 42.1063°	Non-mappable travertine body (small extent and thickness), partly buried under Holocene alluvial plain; deposit is slightly inclined towards Tiber valley, and characterised by massive facies. Nearest mineralised spring, at Cretone, is about 5 km SE of this outcrop	T15a	Massive	24.50	8.83	
			T15b	Massive	23.54	8.61	Calcite
			T15c	Massive	24.48	7.75	
			T15d	Massive	23.50	8.82	
16	Poggio degli Ulivi Lat: 12.6471° Long: 42.2340°	Gently inclined outcropping terrace, about 10 m thick, mainly composed of phytoclastic facies, poorly coherent in upper portion. Samples T16a and T16b came from lower elevation (less soft and porous) with respect to sample T16. Site may be interpreted as a slope deposit, perhaps laterally or vertically transitional with waterfall and pool association	T16	Phytoclastic, very soft and porous	25.05	−0.21	
			T16a	Phytoclastic	26.92	−7.83	
			T16b	Phytoclastic	26.18	−8.39	

Table 1 (continued)

ID	Site	Site description	Sample	Sample description	$\delta^{18}O$ ‰ VSMOW	$\delta^{13}C$ ‰ VPDB	Mineralogy
18	Ponte Ferrovia Lat: 12.6227° Long: 42.2187°	Fossil travertine cliff, ~10 m high (Fig. 5b). Three facies were identified: phytoclastic, stromatolitic, and coated grains. Deposit is interpreted as related to a waterfall environment	T18a	Phytoclastic	24.24	0.84	
			T18b	Phytoclastic	24.40	−0.50	
19	Ponte Sfondato Lat: 12.6463° Long: 42.2105°	Deposit of well-bedded, tabular, calcareous silty material exposed along a road cross section, ~15 m high. Layer of coated grains found in a silty matrix. Low-energy environment, distal from source area (probable floodplain)	T19	Coated grains, in a silty matrix	25.22	−3.45	Calcite + Quartz (10%)
20	Prima Porta Lat: 12.5047° Long: 42.0136°	Travertine body lies below ~ 8 m of alluvial sediment of Tiber; 6 samples from drilled cores were collected at various depths. Massive travertine layers are slightly inclined. Water and free gases were collected from well	T20-8E	Massive	27.52	11.42	Calcite
			T20-9L	Massive	27.44	11.65	Calcite
			T20-9Z	Massive	27.76	11.06	
			T20-10O	Massive	27.51	11.00	Calcite
			T20-11G	Massive	27.89	11.54	
			T20-11R	Massive	28.17	11.82	Calcite
21	Ponzano Lat: 12.5640° Long: 42.2608°	Deposit of calcareous sand exposed along a road cross section. Deposit is ~ 25 m high; sand is well-bedded, with planar cemented layers containing calcareous nodules and tubules. Probable floodplain environment	T21a	Nodule	26.78	−4.90	Calcite + Quartz (10%)
			T21b	Tubule	27.11	−6.37	
			T21	Calcareous sand	n.a	n.a	Quartz (40%) + Phyllosilicates (30%) + Calcite (20%) + Feldspars (10%)
23	Valle Giulia Lat: 12.4795° Long: 42.9182°	Travertines outcrop along vertical slope in north-central Rome, above river gravels and sands. Phytoclastic and phytohermal travertines, calcareous phytoclastic sands and sandy silts of predominantly fluvio-palustrine environment are main facies identified. Stromatolitic facies and thin layers of yellow-brownish laminae, sometimes with semi-translucent calcite veins, indicate a waterfall environment	VG1	Phytoclastic	24.21	2.62	Calcite + Quartz (<5%)
			VG2	Phytoclastic	24.27	4.15	
			VG3	Stromatolitic laminae	24.04	4.78	
			VG4	Phytoclastic	24.13	3.73	
			VG5	Phytoclastic	24.24	3.69	
			VG6	Phytoclastic	23.80	4.48	
			VG7	Phytoclastic	25.02	2.07	
			VG8	Phytoclastic	25.52	4.63	
			VG9	Phytoclastic	24.96	4.22	
			VG10	Stromatolitic laminae	24.68	3.97	Calcite + Quartz (10%)
			BB1	Phytoclastic	25.53	4.73	
			BB2	Phytoclastic	25.07	4.48	

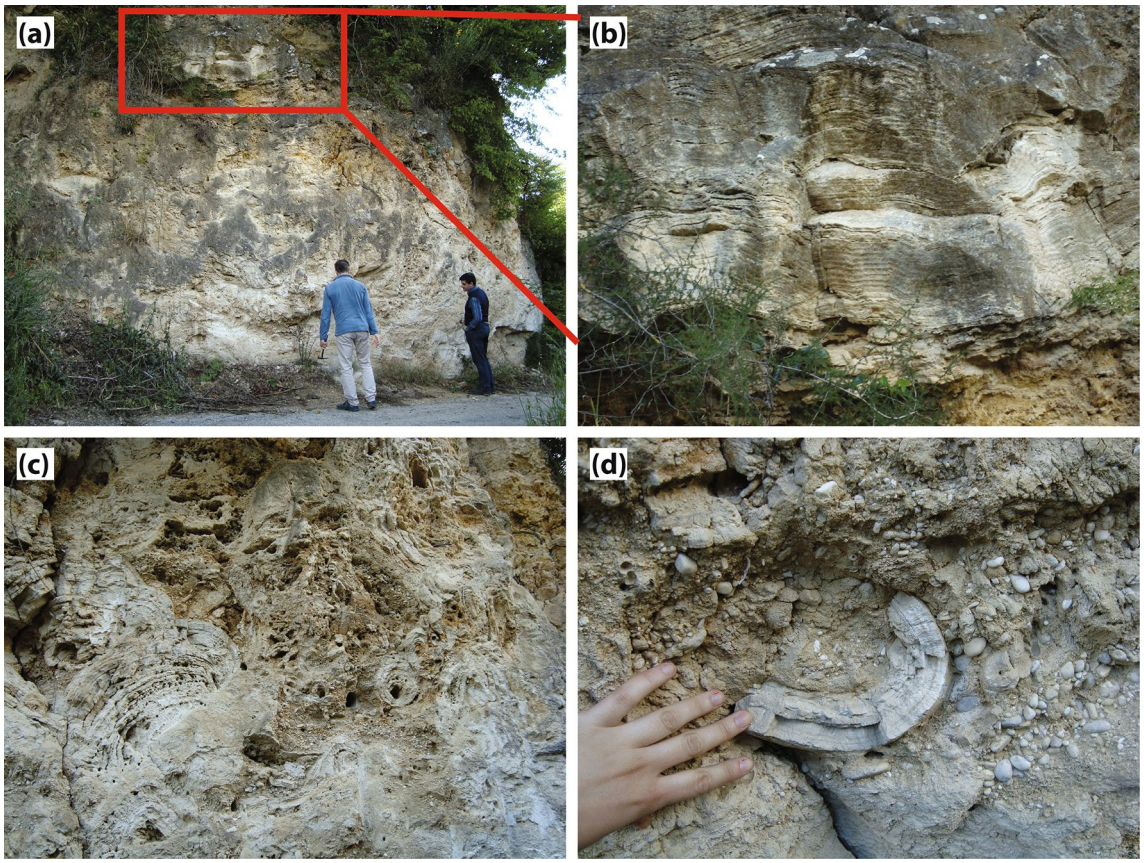

Fig. 5 **a** General view of 'Ponte Ferrovia' site; **b** stromatolitic travertine with sub-horizontal laminae; **c** in the lower-middle part of 'Ponte Ferrovia' site is visible a more 'chaotic' system, with tubules and corrugates laminae; **d** from the same site of (**c**), a travertine tube not completely formed or eroded

in the field of Italian travertine, although their $\delta^{18}O$ values are located towards the area of the most positive values and most carbon isotope data plot towards the higher end of the diagram.

Based on XRD analysis, the studied travertines are composed of almost pure calcite; aragonite was not detected in any sample (Table 1). In the samples from 'Valle Giulia' and 'Ponte Sfondato', a small amount of quartz (lower than 10%) was identified. The sample from 'Ponzano' is composed of quartz (~40%), calcite (~20%), feldspars (~30%), and phyllosilicates (~10%).

Water and gas geochemistry

The $\delta^{18}O_w$ values, chemical compositions, and chemical-physical parameters (T, pH, Eh, EC) of water associated with travertines from 'Acqua Forte', 'Prima Porta', and 'Tivoli' are listed in Table 3. Groundwater can be classified as Ca–HCO_3 and Ca–SO_4–HCO_3, although the 'Prima Porta' sample shows slight enrichment in sodium and chloride; chemical data were used to calculate the Mg/Ca ionic ratio, which ranges between 0.17 and 0.93, because this parameter affects carbonate mineralogy. All waters displayed high electrical conductivity (up to 4250 µS/cm) and a slightly acidic pH, ranging between 6.1 and 6.5. On the basis of their temperatures, the waters from 'Acqua Forte' and 'Prima Porta' are classifiable as 'cold' ($T < 20$ °C) and the remaining samples as warm ($T = 20$–24 °C). The redox potential values (Eh) of the gas vent waters are negative (up to −350 mV in the 'Cretone' sample), with the exception of that from 'Acqua Forte', which shows a slightly positive value (28 mV). The $\delta^{18}O_w$ values of groundwaters range from −6.2 to −7.3‰ and are compatible with the isotope composition of local meteoric water (Giustini et al. 2016).

The 'Acqua Forte', 'Prima Porta', and 'Tivoli' sites exhibit vigorous-free gas emission, identified as CO_2-dominated according to the chemical composition of free gases. The carbon isotopic composition of this CO_2 ranges from −0.51 to −2.86‰ vs. VPDB, with the $\delta^{13}C_{CO2}$ values of the 'Acqua Forte' and 'Prima Porta' gas vents slightly higher (−0.51 and −0.68‰, respectively) than those measured in the Tivoli area (~−2.8‰) (Table 3). Despite such differences, all these values are comparable with the $\delta^{13}C$ of several CO_2-dominated gas vents in central Italy, the origin of which

Table 2 Mean values of stable oxygen and carbon isotope compositions and relative standard deviations (σ) of travertines in the Tiber valley

ID	Site	Type	Long	Lat	Elevation m a.s.l.	*N*	$\delta^{18}O$ ‰ VSMOW	σ	$\delta^{13}C$ ‰ VPDB	σ	$\delta^{13}C_{parental\ CO2}$ ‰ VPDB	Age (ka)
1	Acqua Forte	Phytoclastic	42.2872	12.5303	35	2	25.94	0.63	10.61	1.50	2.23	
2	Cascata	Stromatolitic/phytoclastic	42.2230	12.6201	49	4	24.69	0.13	−1.89	0.96	−12.77	
3	Castiglione in Teverina[a]	Phytoclastic	42.6822	12.1990	210	1	26.00		8.10		−0.78	
4	Cava Casa dei Preti	Nodules and tubules	42.1752	12.6398	51	2	24.37	0.06	−2.47	0.98	−13.47	
5	Cerdomare-Poggio Moiano[a,b]	Massive	42.2112	12.8362	373	5	24.37	0.92	3.52	1.07	−6.28	
6	Civita Castellana[a]	Massive	42.2600	12.4516	150	4	23.25	1.66	7.33	1.11	−1.71	133[d]
7	Civitella d'Agliano[a]	Phytoclastic	42.6085	12.2121	140	1	25.90		9.00		0.30	
8	Ferento[a]	Phytoclastic	42.4879	12.1326	275	1	25.70		6.70		−2.46	
9	Fiano Romano	Phytoclastic	42.1423	12.5898	75	5	25.16	1.21	6.90	2.08	−2.22	170[e]
10	Grotta Marozza[a]	Phytoclastic	42.0653	12.6552	125	1	25.30		0.20		−10.26	
11	Grotte S. Stefano[a]	Phytoclastic	42.5067	12.2159	230	1	26.50		7.40		−1.62	
12	Orte I[a]	Massive	42.4634	12.3660	70	2	24.40	0.57	6.40	0.85	−2.82	
13	Orte II[a]	Massive	42.4530	12.3565	220	6	22.74	0.94	8.18	0.15	−0.68	
14	Osteria Morricone[a]	Massive	42.1082	12.6911	120	1	23.90		6.90		−2.22	
15	Piana Bella	Massive	42.1063	12.6358	40	4	24.00	0.56	8.50	0.51	−0.30	
16	Poggio degli Ulivi	Phytoclastic	42.2340	12.6471	95	3	26.05	0.94	−5.47	4.57	−17.07	
18	Ponte Ferrovia	Phytoclastic	42.2187	12.6227	53	2	24.32	0.11	0.17	0.95	−10.29	
19	Ponte Sfondato	Coated grains	42.2105	12.6463	77	1	25.22		−3.45		−14.63	
20	Prima Porta	Massive	42.0136	12.5047	18	6	27.71	0.28	11.42	0.33	3.20	
21	Ponzano	Nodules and tubules	42.2608	12.5640	155	2	26.95	0.24	−5.64	1.04	−17.26	
22	Tivoli[c]	Massive	41.9625	12.7382	60	31	24.94	0.60	9.54	0.68	0.95	134.8–219.5[b]
23	Valle Giulia	Phytoclastic/stromatolitic	41.9182	12.4795	27	12	24.62	0.59	3.96	0.84	−5.74	

The carbon isotope compositions of parental CO_2 are calculated by means of Panichi and Tongiorgi equation (1976)

[a]Data from Manfra et al. (1976)

[b]Data from Minissale et al. (2002)

[c]Data from De Filippis et al. (2013)

[d]Data from Tuccimei et al. (2001)

[e]Data from Faccenna and Funiciello (1993)

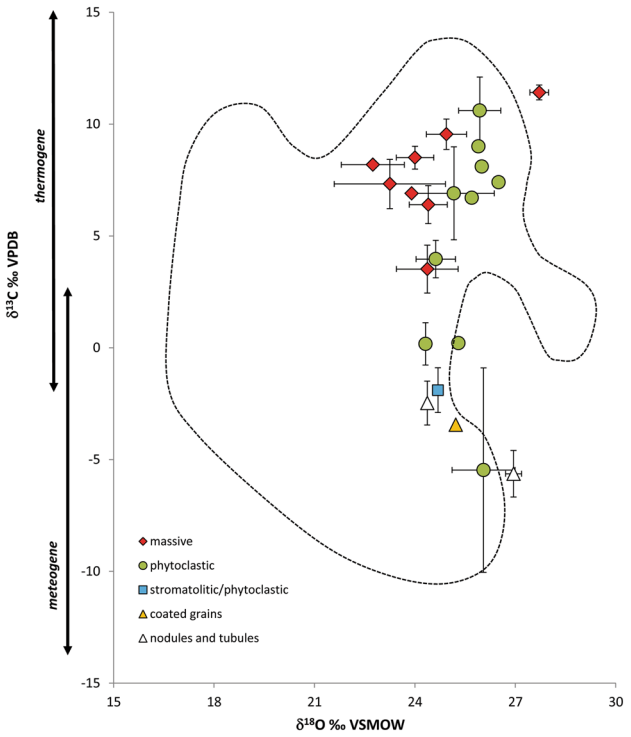

Fig. 6 Stable oxygen and carbon isotope compositions of different travertine facies in the Tiber valley (*error bars* indicate the standard deviation). $\delta^{18}O$ and $\delta^{13}C$ of travertines of central-southern Italy (data after Ascione et al. 2013; Raimondi et al. 2015; Vignaroli et al. 2016; Minissale 2004 and reference therein) are represented by the field drawn with *dashed line*

is generally ascribed to a mixture of mantle-degassing and limestone decarbonation in varying proportions (Chiodini et al. 2004; Minissale 2004).

Discussion

Carbon-stable isotopes and origin of CO_2

Stable isotope analyses have turned out to be important in improving our understanding of the genesis of travertines (Friedman 1970; Turi 1986; Andrews et al. 1997; Fouke et al. 2000; Minissale et al. 2002; Uysal et al. 2007; Kele et al. 2008, 2011). In particular, carbon and oxygen isotope data can help to determine the origin of parental CO_2 and precipitation conditions (temperature and isotope composition of precipitation water), respectively.

The carbon isotopic composition of travertine is primarily controlled by the $\delta^{13}C$ values of possible CO_2 sources. These sources (and their $\delta^{13}C$ values) may be atmospheric ($\delta^{13}C \sim -8‰$ VPDB), organic (generally lower than −20‰ VPDB; Cerling et al. 1991), or derived from limestone decarbonation, which generates CO_2 with $\delta^{13}C = -1$ to +2‰ VPDB (Turi 1986), and mantle/magma which releases CO_2 with $\delta^{13}C = -5$ to −8‰ VPDB (Javoy et al. 1986). As the $\delta^{13}C$ ranges of the various CO_2 sources are greater than that induced by fractionation during travertine deposition, carbon isotopic compositions can provide insights into the origins of fossil travertine CO_2 (Minissale et al. 2002). However, problems such as incorrect identification may arise due to mixing; secondary processes may have a further impact on the carbon isotope composition of the precipitating carbonate, such as CO_2 degassing or biogenic activity, especially downstream of spring vents (Fouke et al. 2000; Kele et al. 2011). Such processes generally result in the preferential loss of light isotopes and the consequent increase in the $\delta^{13}C$ of the carbonate rock (Fouke et al. 2000; Kele et al. 2011). The effect of microbial activity is still subject to debate and may produce carbon fractionation with either positive or negative shifts with respect to equilibrium value (Guo et al. 1996; Fouke et al. 2000; Andrews 2006); photosynthesis preferentially removes $^{12}CO_2$ from water, leaving calcite enriched up to 6‰ of ^{13}C (Guo et al. 1996).

On the basis of carbon isotope data, and according to the classification of Pentecost (2005), both thermogene and meteogene travertines were identified along the Tiber valley (Fig. 6). The thermogenic type includes both massive and phytoclastic macroscopically distinguishable varieties of travertine, indicating that carbon isotopes are not closely connected with the lithofacies, whereas meteogene travertines consist of phytoclastic, stromatolitic facies and coated grains, nodules, and tubules, indicating the progressive input of organic CO_2. Thermogenic travertines with phytoclastic facies may also be defined as 'travitufa', representing samples precipitating from cooled hydrothermal waters, away from the spring orifice. They have a porous aspect and contain abundant fragments of plants, but their isotopic signature indicates carbon dioxide of deep origin. Most of the samples exhibit carbon isotopic compositions more positive than +7‰ VPDB, values which may be explained not only by the deep origin of carbon but also environmental factors, especially CO_2 degassing, in view of the fact that travertines are probably not always sampled close to the spring orifice.

The $\delta^{13}C$ values of some samples fall in the intermediate range of thermogenic and meteogenic travertine (−2/+3‰ VPDB), suggesting that a mix of inorganic CO_2 and soil CO_2 generated by plant respiration (practically ubiquitous) may have occurred.

The empirical equation

$$\delta^{13}C_{\text{parental } CO_2} = 1.2 \times \delta^{13}C_{\text{travertine}} - 10.5 \quad (1)$$

proposed by Panichi and Tongiorgi (1976) calculates the $\delta^{13}C$ of CO_2 released from water during travertine deposition ($\delta^{13}C_{\text{parental } CO_2}$) at the spring orifice. The calculated carbon isotopic compositional range for parental CO_2 varies

Table 3 Chemical and oxygen isotope composition of water samples and carbon isotope composition of free gases associated with mineralised waters

ID	Site	Long	Lat	T (°C)	pH	EC (µS/cm)	Eh (mV)	Ca (mg/L)	Mg (mg/L)	Na (mg/L)	K (mg/L)	HCO_3 (mg/L)	SO_4 (mg/L)	Cl (mg/L)	Mg/Ca	$\delta^{18}O_w$ (‰ VSMOW)	$\delta^{13}C_{CO2}$ (‰ VPDB)
1	Acqua Forte	42.2872	12.5303	17	6.53	3865	28	804	102	102	14	956	1500	141	0.21	−6.82	−0.51
20	Prima Porta	42.0136	12.5047	18	6.15	3080	−7.4	460	47	146	203	1831	302	58	0.17	−6.18	−0.68
25	Tivoli-Bamboo	41.9451	12.7380	24	6.24	2608	−255	248	139	93	17	464	786	144	0.93	−7.28	−2.86
26	Tivoli-Lago Regina	41.9671	12.7211	20	6.10	3280	−210	367	145	103	15	945	764	147	0.65	−6.49	−2.69
27	Cretone	42.0845	12.6931	23	6.22	4250	−350	756	164	195	11	1658	1189	515	0.37	−7.26	

T temperature, *EC* electrical conductivity, *Eh* redox potential

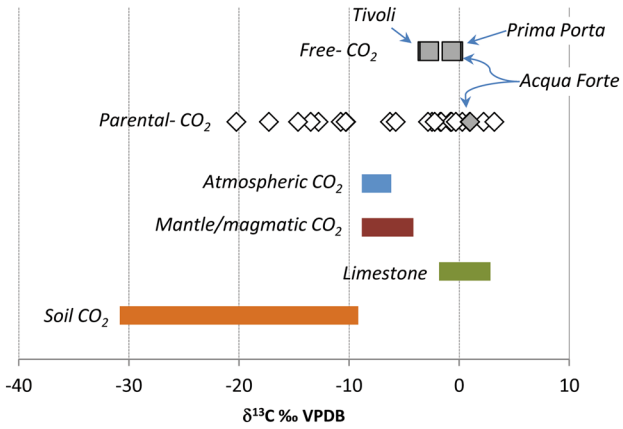

Fig. 7 Carbon isotopic composition of parental CO_2 calculated by Panichi and Tongiorgi equation (1976) (*white diamonds*), and free gases associated with 'Prima Porta', 'Acqua Forte', and 'Tivoli' sites (*grey squares*). *Grey diamond* represents the parental CO_2 calculated for the spring's orifice sample from 'Acqua Forte' site. Ranges of $\delta^{13}C$ values of possible CO_2 sources are from Clark and Fritz (1997)

between ~−20 and ~+3‰ (Table 2; Fig. 7). The position of the spring orifice of most of the studied travertines is unknown, i.e., we cannot exclude the possibility that they were not affected by secondary effects (which generally tend to increase the $\delta^{13}C$ of the travertine), so that Eq. (1) generally overestimates the $\delta^{13}C$ of the parental carbon dioxide. Despite this limitation, thermogenic travertines show values of parental CO_2 in the range of −6 to +3‰, matching the $\delta^{13}C$ of CO_2 of the present-day gas vents in the Tyrrhenian sector of central Italy ($\delta^{13}C$ −9 to +2‰ VPDB; Minissale 2004), whose origin may be ascribed to varying proportions of both mantle/magma degassing and limestone decarbonation (Chiodini et al. 2004; Minissale 2004). The $\delta^{13}C$ of free gases associated with the 'Prima Porta', 'Acqua Forte' and 'Tivoli' sites also falls within the range of the values of the gas vents of central Italy (Table 3; Fig. 7); the first two show ^{13}C-enrichment probably due to a lower percentage of mantle-degassing and/or biogenic CO_2 input, compared with the CO_2 gas emissions of the upper Tiber valley (Vaselli et al. 1997) and the Tivoli area. Comparing $\delta^{13}C_{parental\ CO_2}$ with the isotope composition of free gases associated with the 'Prima Porta' and 'Tivoli' sites (Table 3; Fig. 7), a significant difference appears ($\delta^{13}C_{parental\ CO2}$ is about 4‰ enriched in ^{13}C with respect to free gases). This discrepancy may partly be attributed to the overestimation above-mentioned for Eq. (1), indicating that the samples were located at a certain distance from the spring orifice (Fouke et al. 2000; Kele et al. 2008, 2011). In the case of the 'Acqua Forte' site, where the travertine sample was collected from the spring orifice, the ^{13}C enrichment is lower (~1.5‰).

Variable amounts of soil CO_2 are considered to be responsible for the observed variations in travertine

$\delta^{13}C_{parental\ CO_2} < -10‰$ VPDB. In fact, the biogenic CO_2 originating in the soil may be transferred to shallow groundwater, due to the high permeability of the alluvial deposits of the Tiber valley. In addition, even a small contribution of this organic CO_2 can greatly affect the final isotopic composition of CO_2 because of its low ^{13}C content ($\delta^{13}C_{organic} < -20‰$ VPDB; Cerling et al. 1991).

Oxygen stable isotopes and calculation of palaeo-temperature of water

The oxygen isotope composition of the Tiber valley travertines has a relatively large variability ($\delta^{18}O = +21.90$ to $+27.71‰$ VSMOW), although most of the samples fall within a narrower range between +24 and +25‰ VSMOW. Thermogenic travertines show greater variability than meteogenic deposits, although the mean $\delta^{18}O$ values of the two groups are very similar, at +25.05‰ and +25.35‰ VSMOW, respectively (Fig. 6). The phytoclastic, stromatolitic facies, and samples of coated grains, nodules, and tubules are generally characterised by higher oxygen values than massive travertines, indicating that phytoclastic stromatolitic facies form at lower temperatures.

In general, the relatively wide-ranging $\delta^{18}O$ values of the travertines indicate precipitation from isotopically different waters at varying temperatures. Precipitation temperature can be calculated if the oxygen isotope compositions of the carbonate and the water of deposition are known values, which in this case must be assumed. The water oxygen isotope value may be that typical of meteoric origin, represented by the water analysed at 'Acqua Forte', 'Prima Porta', and the Tivoli area, i.e., −6‰/−7‰ VSMOW (Table 3). Crucial assumptions must be made about isotopic equilibrium and the selection of one of the calcite–water equations relating oxygen isotopes to temperature. It is currently unclear which, if any, of the published calibration equations, represents true equilibrium. It is also unclear precisely in which travertine facies calcite precipitates at equilibrium. Kele et al. (2015) contend that very little or no fractionation due to kinetic effects occurs close to the spring vents or in pools; vent and pool travertines show higher mineral-water oxygen isotope fractionation than the values reported by Kim and O'Neil (1997), whereas many of them fit the curves published by Coplen (2007), Tremaine et al. (2011), and Affek and Zaarur (2014). In the present study, one of the equations reported by Kele et al. was selected to calculate the range of water temperatures at the time of precipitation by means of the oxygen isotopic composition of travertine:

$$1000\ln\alpha_{CaCO_3-H_2O} = 17\frac{10^3}{T} - 26, \quad (2)$$

where $\alpha_{CaCO_3-H_2O}$ is the fractionation factor between calcite and water, and T is the temperature in K. The temperature ranges from 5 to 35 °C, with an average of about 20 °C (Table 4). This approach does not take into account the different facies represented by the samples of this study, i.e., kinetic effects and enrichment of ^{18}O downstream because of water evaporation (especially evident in sub-aerial precipitation). These effects would produce a higher isotopic composition of the carbonate and consequently a lower temperature. The temperatures listed in Table 4 must be considered possible minimum estimates of the true values. A comparison of the calculated temperatures and those measured at 'Acqua Forte', which was the only active depositing spring sampled in this study, reveals that Eq. (2) estimates this context quite well: the oxygen isotope compositions of the spring water and travertine, which were −6.82 and +25.49‰, respectively, give a deposition temperature of 16.4 °C, which matches the directly measured temperature of 17 °C.

The calculated temperatures are approximately consistent with those recorded in mineralised groundwaters sampled in the Tiber valley. A temperature as low as 5 °C,

Table 4 Palaeo-temperatures of formation of Tiber valley travertines

ID	Site	*A* $\delta^{18}O$ ‰ VSMOW	*B* *T* °C (Eq. 2)	*C* *T* °C measured
1	Acqua Forte	25.94	13–18	17
2	Cascata	24.69	19–25	
3	Castiglione in Teverina[a]	26.00	13–18	
4	Cava Casa dei Preti	24.37	21–26	
5	Cerdomare-Poggio Moiano[a,b]	24.37	21–26	
6	Civita Castellana[a]	23.25	27–32	
7	Civitella d'Agliano[a]	25.90	14–19	
8	Ferento[a]	25.70	15–20	
9	Fiano Romano	25.16	17–22	
10	Grotta Marozza[a]	25.30	16–22	
11	Grotte S. Stefano[a]	26.50	11–16	
12	Orte I[a]	24.40	21–26	
13	Orte II[a]	22.74	29–35	
14	Osteria Morricone[a]	23.90	23–29	
15	Piana Bella	24.00	23–28	
16	Poggio degli Ulivi	26.05	13–18	
18	Ponte Ferrovia	24.32	21–27	
19	Ponte Sfondato	25.22	17–22	
20	Prima Porta	27.71	5–10	18
21	Ponzano	26.95	9–13	
22	Tivoli[c]	24.94	18–23	20–24
23	Valle Giulia	24.62	20–25	

[a]Oxygen isotope compositions of travertines

[b]Temperatures calculated using Eq. (2) from Kele et al. (2015)

[c]Measured temperatures of the waters associated with travertines

that recorded for the 'Prima Porta' spring, which is associated with a typically thermogenic fossil travertine, may be the result of those isotopic effects which lower the true temperature.

Of note is the striking correspondence of the temperatures calculated and directly measured for the hydrothermal springs of the Tivoli area (also called the Acque Albule springs) (Table 4), which contributed to the precipitation of the large 'tiburtinus' plateau. Several hydrogeological and geochemical studies have been carried out in this context (e.g., Petitta et al. 2011; Carucci et al. 2012), highlighting the fact that deep high-salinity groundwater, rising along tectonic lines, mixes with shallow fresh groundwater, decreasing the temperature of the water in the travertine aquifer. A similar model may be depicted for the Tiber valley because of the large capacity of the shallow aquifer hosted in the alluvial deposits.

The above palaeo-temperature calculations do not take into account the possibility that the water cycle in the area may have varied in the past, particularly during colder periods when the $\delta^{18}O$ values of palaeo-spring waters were lower than those presently existing as a temperature effect on isotope fractionation in precipitation. In this case, the calculated temperatures may be further overestimated, taking into account that a 1‰ difference in $\delta^{18}O_{water}$ corresponds to a difference in water temperature of about 5 °C, according to the equation of Kele et al.

The range of temperatures calculated for the Tiber valley travertines indicates that the thermogenic travertines were formed by slightly thermal water (at a temperature more than 5 °C above the mean annual air temperature, according to the definition of Goldscheider et al. 2010) and not by hot springs (>37 °C; cfr. Pentecost 2005), which are often related to thermogenic deposits.

A further constraint for the water temperature at the time of precipitation is the mineralogical composition of the travertines, which are almost pure calcite. Several studies (Friedman 1970; Sturchio 1990; Folk 1994; Fouke et al. 2000) have demonstrated that aragonite usually forms at temperatures ranging from 30 to 60 °C, although particular cases of pure calcite precipitation have been detected at high water temperatures (~67 °C), especially when the precipitation rate was observed to be high (Jones et al. 1996; Kele et al. 2008). In the Tiber valley travertines, the absence of aragonite indicates that carbonate precipitation occurred from waters with temperatures lower than 30 °C, as also indicated by the isotope data. In addition, according to Fischbeck and Müller (1971), aragonite precipitation becomes significant when the water Mg/Ca ratio is ~2.9; in our water samples, this ratio is lower than 0.9 (Table 3).

Travertines, tectonic activity, and palaeo-environmental remarks

The geochemical features and depositional characteristics of travertines are controlled by the balance between several factors, including tectonic/seismic activity, climatic variations, fluid discharge, chemical composition of travertine-depositing waters, mixing of deeply derived waters and shallow waters, CO_2 levels, and microbiological activity.

Travertine deposition is common in areas affected by extensional tectonics, where the circulation of fluids which have the potential for travertine deposition is controlled by damage zones resulting from normal faulting (Altunel and Hancock 1993; Çakır 1999; Brogi 2004; Altunel and Karabacak 2005; Uysal et al. 2007; Mesci et al. 2008; Selim and Yanık 2009; Kele et al. 2011; De Filippis et al. 2012; Brogi et al. 2012, 2014; Özkul et al. 2013, 2014; Van Noten et al. 2013). In contrast, travertine precipitation along major strike-slip fault zones is less common and/or studies examining travertines related to strike-slip faulting are limited (Faccenna et al. 2008; Temiz et al. 2013; Çolak Erol et al. 2015). To clarify the relationship between tectonics and travertines (and consequently between tectonics and the origin of CO_2-rich fluids) along the Tiber valley, Fig. 8 shows the spatial distribution of meteogenic and thermogenic travertines in the study region. It is evident from this geological sketch that most of the thermogenic travertines ($\delta^{13}C > +0.5‰$) are distributed along the border of the main volcanic districts and are aligned along the NNW–SSE-oriented normal faults which compose the structure of horsts/grabens in this area (Funiciello and Parotto 1978; Faccenna and Funiciello 1993). Out of this aligned distribution, the 'Fiano Romano' and 'Prima Porta' thermogenic travertines seem to be directly connected to the Pleistocene N–S strike-slip shear zone, south of the Monte Soratte structure, already partially described by Faccenna (1994). In contrast, the 'Cerdomare' deposit (site 5, Table 2) is the most eastern thermogenic travertine and outcrops for about 4 km in the Apennine direction, along the southern edge of an intramontane basin within the Meso-Cenozoic limestone of the Sabini–Lucretili–Tiburtini Mountains, and probably related to the rise of deep fluids migrating through a normal buried fault (Manfra et al. 1976).

In the present study, matching other cases in the literature, most of the travertine deposits occur along the normal faults of the Tiber graben, although a few interesting examples ('Prima Porta', 'Fiano Romano', and the well-known 'Tivoli' deposit) seem to be related to strike-slip faulting.

The close spatial relationship between faults, thermogenic travertine deposits, current gas emissions, and mineralised groundwaters, in general, have demonstrated that tectonic discontinuities, which are common in deformed carbonate bedrock, are natural pathways allowing meteoric waters to

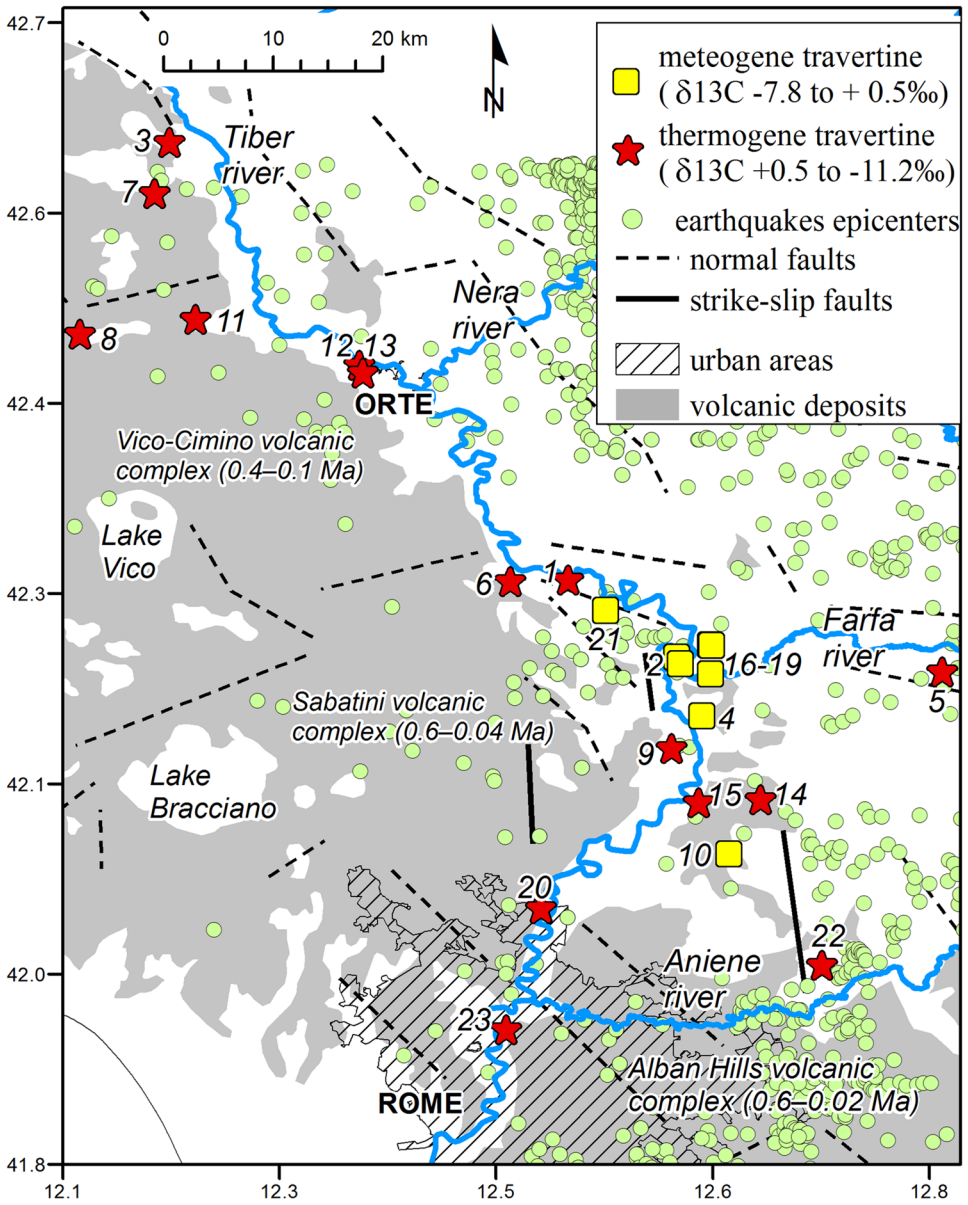

Fig. 8 Location map of meteogene ($\delta^{13}C$ from −7.8 to +0.5‰, *yellow squares*) and thermogene ($\delta^{13}C$ from +0.5 to +11.2‰, *red stars*) travertines and of low-magnitude earthquakes ($M < 5$) epicenters recorded in the 2005–2015 period at shallow and deep crustal levels (up to 30-km depth) (Italian Seismological Instrumental and parametric Data-basE ISIDE, http://iside.rm.ingv.it, last accessed May 2015)

descend into the subsurface and hydrothermal fluids to rise to the surface. As a consequence, the presence of thermogenic travertine may indicate the migration of deep-seated gases, probably associated with warm, saline waters, that is generally conveyed towards the surface by tectonic discontinuities. The precipitation of mineral species such as calcite, oxides, and silica from supersaturated hydrothermal fluids may take place over hundreds of years, decreasing the permeability of these tectonic structures (Sibson 1987); however, fluid circulation can be guaranteed by persistent faulting and fracturing, which progressively open new conduits for fluid flow, as implied by tectonic activity (Brogi et al. 2010, 2012). In this regard, the fact that the Tiber valley springs have remarkable saline contents would imply that the tectonic fissures could be sealed by mineral deposition; this sealing process may be effectively contrasted by the recent activity of the related faults. The diffuse present-day seismicity recorded by the low-magnitude earthquakes ($M < 5$) in the study area (Fig. 8) may corroborate the view that tectonic activity allowed tectonic fissures to remain open and maintain mineralised fluid circulation.

The relationship between the Tiber valley travertine deposition, volcanic activity, and glacial/interglacial cycles was explored by comparing the ages of the travertines with the main eruptive events of the nearby volcanic districts, as well as with palaeo-climatic indicators (Fig. 9). As previously mentioned, the travertines sampled in this study belong to Middle Pleistocene lithostratigraphic units and were stratigraphically positioned at about 550–500 and 400–200 ka; the most recent travertine outcrops have been referred to the

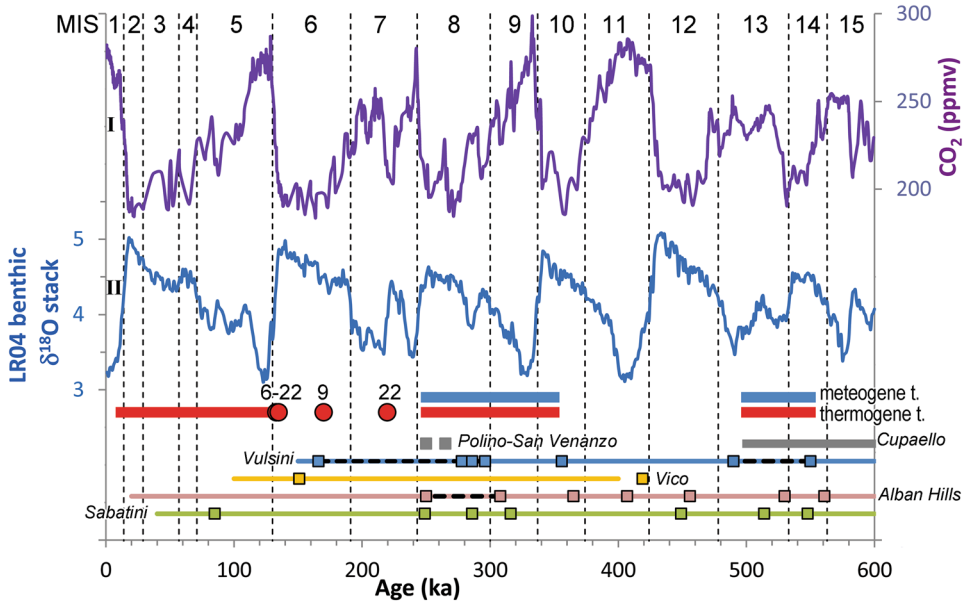

Fig. 9 Comparison between travertine dating (Faccenna and Funiciello 1993; Tuccimei et al. 2001; Minissale et al. 2002; Mancini et al. 2004), volcanic activity, and palaeoclimate indicators. Curves I and II represent atmospheric carbon dioxide-level variations (Luthi et al. 2008) and LR04 benthic isotope stack record (Lisiecki and Raymo 2005); Marine Isotope Stages (MIS) were defined by Lisiecki and Raymo (2005). Time-frame of volcanic activity of the Roman Province (Peccerillo 2003) and intra-Apennine volcanic centres (Laurenzi et al. 1994) is shown; *square symbols* represent the age of main eruptive events (Perini et al. 2004; Marra et al. 2009; Palladino et al. 2010; Sottili et al. 2010)

Late Pleistocene and Holocene (Mancini et al. 2004; Fig. 9). Radiometric U-Th dating is available in the literature for the 'Civita Castella', 'Fiano Romano', and 'Tivoli' deposits (133, 170, and 134.8–219.5 ka, respectively; Faccenna and Funiciello 1993; Tuccimei et al. 2001; Minissale et al. 2002) (Table 2).

Figure 9 shows the variation in atmospheric CO_2 levels, the $\delta^{18}O$ climatic stack curve from deep sea cores, the time range of large-scale volcanic events in the Roman Province (distinguished by volcanic districts), and the depositional time range of the studied travertines for the last 600 ka. It is evident that the time-frame of travertine formation is so approximate that it barely allows definite associations between climatic/volcanic events and travertine deposition to be identified. However, Fig. 9 does provide certain indications. First, the most recent travertines are entirely thermogenic; their formation is correlated with the last intense Sabatini event and does not show any clear correspondence with climatic phases, which alternate between glacial and interglacial from 200 ka towards the Last Glacial Maximum. As regards the travertines deposited during the periods 350–250 and 550–500 ka, both thermogenic and meteogenic deposits were recorded, corresponding to the intense volcanic phases of most of the Latium volcanic complexes, especially the main eruptions of the Sabatini complex, indicating a relationship between events in that area and the development of travertine springs. The climatic relationship again seems uncertain, since the time-span of formation of any travertine corresponds to both glacial and interglacial climatic conditions (travertines formed between 350–250 ka encompass the MIS 8 and 9 glacial/interglacial, and those formed between 550–500 ka the MIS 13–14 glacial/interglacial couple). Recent studies (Frank et al. 2000; Faccenna et al. 2008; De Filippis et al. 2013) have shown that the formation of travertine depends on climatic factors, particularly variations in aridity and humidity. These studies contend, for instance, that thermogenic travertine deposition may be reduced in arid glacial periods, due to scarce water seepage at deeper levels and consequent decreased hydrothermal circulation. Conversely, in the warm humid periods of interglacial stages, travertine deposition may be favoured by the increased availability of water which facilitates deep-shallow water mixing, as in the case of the Tivoli deposits. However, this general response of travertine development to climate is less obvious in our study.

Considering the above evidence, Fig. 10 shows a possible palaeo-environmental reconstruction of the middle Tiber valley. Corresponding to the structural discontinuities, which intersect the carbonate bedrock and define the Tiber graben, CO_2-rich fluids of deep origin (metamorphic and partly mantle/magma degassing, as revealed by carbon isotopes) found suitable routes for their ascent to the surface, where they mixed with shallow groundwaters. The thermal nature of the deep fluids may be partly obscured

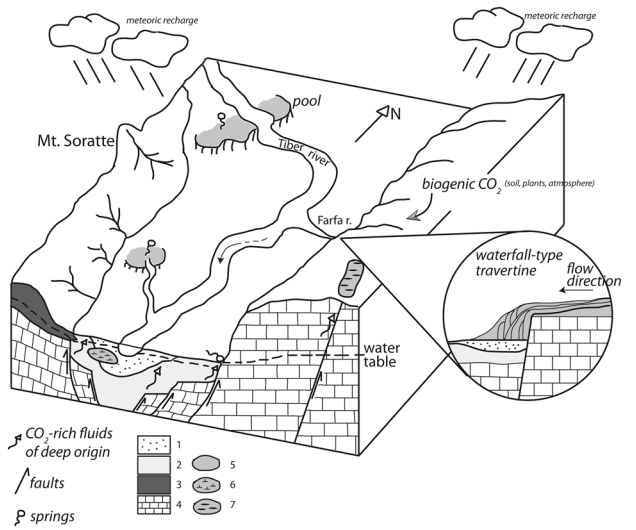

Fig. 10 Schematic palaeo-environmental reconstruction (not to scale) of the middle Tiber valley. *1* Alluvial deposits, *2* Plio-Pleistocene marine and continental deposits, *3* pyroclastic rocks, *4* Meso-Cenozoic limestone, *5* travertine, *6* travertine body buried under the recent alluvial deposits, *7* travertine deposits east of valley (e.g., 'Poggio Moiano/Cerdomare', site n.5, Table 2) related to the rising of deep fluids

by large volumes of cold regional, alluvial, and volcanic aquifer waters, as indicated by the temperature estimation based on travertine oxygen isotopes, and by direct measurement of mineralised spring waters dispersed in the valley; these spring waters consequently often show a hypothermal character. At the points of spring emergence, large travertine bodies were formed by precipitation from supersaturated, CO_2 degassing waters, and eventually grew to form natural dams, upstream of which lacustrine and palustrine pools formed and the related lithofacies were deposited. Some deposits were later buried under the recent alluvial deposits and are thus hidden along the valley.

In this reconstruction, meteogenic travertines were solely formed at the palaeo-confluence of the Farfa and Tiber rivers, on the present-day left bank of the Tiber, at the point where it bends (Fig. 10). These travertines are located on both banks of the Farfa at higher elevations than the present-day banks, and represent a high-energy environment: the association of facies (Fig. 4) attributes these travertines to a sedimentary waterfall environment. The fault bordering the graben probably generated a vertical topographic displacement which developed into a waterfall system suitable for carbonate precipitation, the steep topography subsequently being self-generated by travertine development.

Conclusions

Field observations and geochemical analyses of groundwaters, gas emanations, and travertines along the Tiber valley (central Italy) have highlighted both the origin of CO_2-rich fluids, from which the travertines were deposited, and their relationship with the tectonic setting.

The carbon isotopic composition of the travertines, ranging from −8.11 to +11.42‰ vs. VPDB, identifies two groups of deposits and consequently two different sources of CO_2. Thermogenic travertines ($\delta^{13}C \sim >0.5‰$) are related to CO_2 of prevailingly inorganic origin, mainly from limestone decarbonation. These travertines are clearly aligned along, or located close to, the main tectonic structures and active faults, allowing the rapid rise of fluids circulating at depth. In addition, the close spatial relationship between thermogenic travertines, gas emissions, mineralised groundwaters, and faults indicates that the tectonic discontinuities represent local routes of intense deep fluid circulation. According to our data, the ultimate origin of these travertines was affected by the contribution of deeply derived CO_2-dominated fluids to meteorically derived recharge waters, which diluted the solute contents and reduced the deep water temperature; the $\delta^{18}O$ values of these travertines in fact indicate that the calcite was predominantly formed in warm waters, rarely exceeding 30 °C. The spatial distribution of the epicenters of present-day seismic events is consistent with the locations of the most important faults in the study area and with the locations of thermogenic travertines, gas emissions, and mineralised groundwaters, indicating that tectonic activity ensures the ongoing permeability of faults and fractures. Comparison of the time of travertine deposition with the occurrence of the main volcanic and climatic events taking place during the Pleistocene reveals that volcanism, especially the Sabatini volcanic events, may have had an influence in travertine formation that climate may have not, at least at the level of our dating resolution.

In the meteogenic travertines ($\delta^{13}C \sim <0.5‰$), which are located at the confluence of the Tiber with the Farfa, variable amounts of soil CO_2 are considered to be responsible for the observed depletion in ^{13}C. A waterfall system was probably the original sedimentary environment of these travertines, the growth of this morphology probably being favoured by the vertical displacement of a fault bordering the Tiber graben. Oxygen isotopes show that both types of travertines, meteogenic and thermogenic, were formed in warm or slightly thermal waters.

Acknowledgements We thank S. Stellino (DST-Sapienza) for assistance with XRD analysis and G. Capelli for providing travertine samples from "Prima Porta" site. We are grateful to M. Özkul and an anonymous reviewer, for their suggestions and comments.

References

Affek HP, Zaarur S (2014) Kinetic isotope effect in CO_2 degassing: insight from clumped and oxygen isotopes in laboratory precipitation experiments. Geochim Cosmochim Acta 143:319–330

Altunel E, Hancock PL (1993) Morphology and structural setting of Quaternary Travertines at Pamukkale, Turkey. Geol J 28:335–346

Altunel E, Karabacak V (2005) Determination of horizontal extension from fissure-ridge travertines: a case study from the Denizli Basin, southwestern Turkey. Geodin Acta 18:333–342

Andrews JE (2006) Palaeoclimatic records from stable isotopes in riverine tufas: synthesis and review. Earth Sci Rev 75:85–104

Andrews JE, Riding R, Dennis PF (1997) The stable isotope record of environmental and climatic signals in modern terrestrial microbial carbonates from Europe. Palaeogeogr Palaeocl 129:171–189

Ascione A, Iannace A, Imbriale P, Santangelo N, Santo A (2013) Tufa and travertines of southern Italy: deep-seated, fault-related CO_2 as the key control in precipitation. Terra Nova 26:1–13

Barberi F, Buonasorte G, Cioni R, Fiordelisi A, Foresi L, Iaccarino S, Laurenzi MA, Sbrana A, Vernia A, Villa IM (1994) Plio–Pleistocene geological evolution of the geothermal area of Tuscany and Latium. Mem Descr Carta Geol d'It 49:77–135

Barbieri M, Masi U, Tolomeo L (1979) Origin and distribution of strontium in the travertines of Latium (Central Italy). Chem Geol 24:181–188

Boni CF, Bono P, Capelli G (1988) Carta Idrogeologica del Territorio della Regione Lazio—scala 1:250.000. Regione Lazio, Assessorato alla Programmazione, Ufficio Parchi e Riserve, Università degli Studi di Roma "La Sapienza". Dipartimento di Scienze della Terra, Roma

Brogi A (2004) Faults linkage, damage rocks and hydrothermal fluid circulation: Tectonic interpretation of the Rapolano Terme travertines (southern Tuscany, Italy) in the context of Northern Apennines Neogene–Quaternary extension. Eclogae Geol Helv 97:307–320

Brogi A, Capezzuoli E, Aquè R, Branca M, Voltaggio M (2010) Studying travertines for neotectonics investigations: middle–Late Pleistocene syn-tectonic travertine deposition at Serre di Rapolano (Northern Apennines, Italy). Int J Earth Sci 99:1383–1398

Brogi A, Capezzuoli E, Buracchi E, Branca M (2012) Tectonic control on travertine and calcareous tufa deposition in a low-temperature geothermal system (Sarteano, Central Italy). J Geol Soc Lond 169:461–476

Brogi A, Capezzuoli E, Alçiçek MC, Gandin A (2014) Evolution of a fault-controlled fissure-ridge type travertine deposit in the western Anatolia extensional province: the Çukurbağ fissure-ridge (Pamukkale, Turkey). J Geol Soc Lond 171:425–441

Buccino G, D'Argenio B, Ferreri V, Brancaccio L, Ferreri M, Panichi C, Stanzione D (1978) I travertini della bassa valle del Tanagro (Campania): studio geomorfologico, sedimentologico e geochimico. Boll Soc Geol Ital 97:617–646

Çakır Z (1999) Along strike discontinuity of active normal faults and its influence on Quaternary travertine deposition: Examples from western Turkey. Turk J Earth Sci 8:67–80

Capelli G, Mastrorillo L, Mazza R, Petitta M, Baldoni T, Banzato F, Cascone D, Di Salvo C, La Vigna F, Taviani S, Teoli P (2012) Carta Idrogeologica del Territorio della Regione Lazio, scala 1:100.000 (4 fogli). Regione Lazio, S.EL.CA., Firenze

Capezzuoli E, Gandin A, Pedley M (2014) Decoding tufa and travertine (fresh water carbonates) in the sedimentary record: the state of the art. Sedimentology 61:1–21

Carminati E, Doglioni C (2012) Alps vs. Apennines: the paradigm of a tectonically asymmetric Earth. Earth Sci Rev 112:67–96

Carrara C (1994) I travertini di Canino (VT, Italia centrale): elementi di cronolitostratigrafia, di geochimica isotopica e loro significato ambientale e climatico. Quaternario 7:73–90

Carucci V, Petitta M, Aravena R (2012) Interaction between shallow and deep aquifers in the Tivoli Plain (Central Italy) enhanced by groundwater extraction: a multi-isotope approach and geochemical modelling. Appl Geochem 27:266–280

Cavinato GP, De Celles PG (1999) Extensional basins in the tectonically bimodal central Apennines fold–thrust belt, Italy: response to comer flow above subducting slab in retrograde motion. Geology 27:955–958

Cavinato GP, Cosentino D, De Rita D, Funiciello R, Parotto M (1994) Tectonic–sedimentary evolution of intrapenninic basins and correlation with the volcano–tectonic activity in Central Italy. Mem Descr Carta Geol d'It 49:63–76

Cerling TE, Solomon DK, Quade J, Bowman JR (1991) On the isotopic composition of carbon in soil carbon dioxide. Geochim Cosmochim Acta 55:3403–3406

Chafetz HS, Folk RL (1984) Travertines: depositional morphology and the bacterially constructed constituents. J Sediment Res 54:289–316

Chiodini G, Cardellini C, Amato A, Boschi E, Caliro S, Frondini F, Ventura G (2004) Carbon dioxide Earth degassing and seismogenesis in central and southern Italy. Geophys Res Lett 31:L07615

Claes H, Soete J, Van Noten K, El Desouky H, Marques Erthal M, Vanhaecke F, Özkul M, Swennen R (2015) Sedimentology, three-dimensional geobody reconstruction and carbon dioxide origin of Pleistocene travertine deposits in the Ballik area (south-west Turkey). Sedimentology 62:1408–1445

Clark ID, Fritz P (1997) Environmental isotopes in hydrogeology. CRC Press/Lewis Publishers, Boca Raton, FL

Çolak Erol S, Özkul M, Aksoy E, Kele S, Ghaleb B (2015) Travertine occurrences along major strike-slip fault zones: structural, depositional and geochemical constraints from the Eastern Anatolian fault System (EAFS), Turkey. Geodin Acta 27:154–173

Coplen TB (2007) Calibration of the calcite–water oxygen isotope geothermometer at Devils Hole, Nevada, a natural laboratory. Geochim Cosmochim Acta 71:3948–3957

Cosentino D, Cipollari P, Marsili P, Scrocca D (2010) Geology of the central Apennines: a regional review. In: Beltrando M, Peccerillo A, Mattei M, Conticelli S, Doglioni C (eds) The geology of Italy: tectonics and life along plate margins, vol 36(12. doi:10.3809/jvirtex.2010.00223 **(Journal of the Virtual Explorer Electronic Edition)**

De Rita D, Funiciello R, Corda L, Sposato A, Rossi U (1993) Volcanic units. In: Di Filippo M (ed) Sabatini volcanic complex, vol 114. Quaderni della Ricerca Scientifica, C.N.R., Roma, pp 33–79

De Rita D, Faccenna C, Funiciello R, Rosa C (1995) Stratigraphy and volcano tectonics. In: Trigila R (ed) The volcano of the Alban Hills, Roma, pp 33–71

De Filippis L, Faccenna C, Billi A, Anzalone E, Brilli M, Özkul M, Soligo M, Tuccimei P, Villa IM (2012) Growth of fissure ridge travertines from geothermal springs of Denizli Basin, western Turkey. Geol Soc Am Bull 124:1629–1645

De Filippis L, Faccenna C, Billi A, Anzalone E, Brilli M, Soligo M, Tuccimei P (2013) Plateau versus fissure ridge travertines from Quaternary geothermal spring of Italy and Turkey: Interactions and feedbacks between fluid discharge, paleoclimate, and tectonics. Earth Sci Rev 123:35–52

Epstein S, Mayeda TK (1953) Variations of the $^{18}O/^{16}O$ ratio in natural waters. Geochim Cosmochim Acta 4:213–224

Faccenna C (1994) Structural and hydrogeological features of Pleistocene shear zones in the area of Rome (Central Italy). Ann Geofis 37:121–133

Faccenna C, Funiciello R (1993) Tettonica pleistocenica tra il Monte Soratte e i Monti Cornicolani. Il Quaternario 6:103–118
Faccenna C, Funiciello R, Montone P, Parotto M, Voltaggio M (1994) Late Pleistocene strike–slip tectonics in the Acque Albule Basin (Tivoli, Latium). Mem Descr Carta Geol d'It 49:37–50
Faccenna C, Soligo M, Billi A, De Filippis L, Funiciello R, Rossetti C, Tuccinei P (2008) Late Pleistocene depositional cycles of the lapis Tiburtinus travertine (Tivoli, Central Italy): possible influence of climate and fault activity. Glob Planet Change 63:299–308
Faccenna C, Funiciello R, Soligo M (2010) Origin and deposition of the Lapis Tiburtinus travertine. In: Funiciello R, Giordano G (eds) The Colli Albani volcano. IAVCEI Spec. Publ. 3, Geological Society, London, pp 215–228
Ferreri M, Stanzione D (1978) Contributo alla conoscenza geochimica dei travertini campani: travertini di Paestum e della Bassa Valle del Tanagro. Rend Accad Sci Fis Mat Di Napoli IV 45:1–15
Fischbeck R, Müller G (1971) Monohydrocalcite, hydromagnesite, nesquehonite, dolomite, aragonite and calcite in speleothems of the Frankische Schweiz, Western Germany. Contrib Mineral Petrol 33:87–92
Folk RL (1994) Interaction between bacteria, nannobacteria, and mineral precipitation in hot springs of Central Italy. Geogr Phys Quat 48:233–246
Ford TD, Pedley HM (1996) A review of tufa and travertine deposits of the world. Earth Sci Rev 41:117–175
Fouke BW, Farmer JD, Des Marais DJ, Prat L, Sturchio NC, Burns PC, Discipulo MK (2000) Depositional facies and aqueous-solid geochemistry of travertine-depositing hot springs (Angel Terrace, Mammoth Hot Springs, Yellowstone National Park, USA). J Sediment Res 70:565–585
Frank N, Braum M, Hamach U, Mangini A, Wagner G (2000) Warm period growth of travertine during the Last Interglaciation in Southern Germany. Quat Res 54:38–48
Friedman I (1970) Some investigations of the deposition of travertine from hot springs: I. The isotope chemistry of a travertine depositing spring. Geochim Cosmochim Acta 34:1303–1315
Funiciello R, Giordano G (2008) Note illustrative della Carta Geologica d'Italia alla scala 1:50.000, Foglio 347 ROMA. APAT-Servizio Geologico d'Italia, Roma
Funiciello R, Parotto M (1978) Il substrato sedimentario nell'area dei Colli Albani: considerazioni geodinamiche e paleogeografiche sul margine tirrenico dell'Appennino centrale. Geol Romana 17:233–287
Funiciello R, Giuliani R, Marra F, Salvi S (1994) The influence of volcanism and tectonics on Plio-Quaternary regional landforms in the Southeastern Sabatinian area (Central Italy). Mem Descr Carta Geol d'It 49:323–332
Gandin A, Capezzuoli E (2014) Travertine: distinctive depositional fabrics of carbonates from thermal spring systems. Sedimentology 61:264–290
Gibert RO, Taberner C, Sáez A, Giralt S, Alonso RN, Edwards RL, Pueyo JJ (2009) Igneous origin of CO_2 in ancient and recent hot spring waters and travertines from the northern Argentinean Andes. J Sediment Res 79:554–567
Giustini F, Brilli M, Patera A (2016) Mapping oxygen stable isotopes of precipitation in Italy. J Hydrol Reg Stud 8:162–181
Goldscheider N, Mádl-Szonyi J, Eross A, Schill E (2010) Review: thermal water resources in carbonate rock aquifers. Hydrogeol J 18:1303–1318
Gonfiantini R, Panichi C, Tongiorgi E (1968) Isotopic disequilibrium in travertine deposition. Earth Planet Sci Lett 5:55–58
Guo L, Andrews J, Riding R, Dennis P, Dresser Q (1996) Possible microbial effects on stable carbon isotopes in hot-spring travertines. J Sediment Res 66:468–473
Javoy M, Pineau F, Delorme H (1986) Carbon and nitrogen isotopes in the mantle. Chem Geol 57:41–62
Jones B, Renaut RW, Rosen MR (1996) High-temperature (>90 °C) calcite precipitation at Waikite Hot Springs, North Island, New Zealand. J Geol Soc Lond 153:481–496
Karner DB, Marra F, Renne PR (2001) The history of the Monti Sabatini and Alban Hills volcanoes: groundwork for assessing volcani-tecnonic hazards for Rome. J Volcanol Geotherm Res 107:185–219
Kele S, Demény A, Siklósy Z, Németh T, Tóth M, Kovács MB (2008) Chemical and stable isotope composition of recent hot–water travertines and associated thermal waters, from Egerszalók, Hungary: Depositional facies and non-equilibrium fractionation. Sediment Geol 211:53–72
Kele S, Özkul M, Fórizs I, Gökgöz A, Baykara MO, Alçiçek MC, Németh T (2011) Stable isotope geochemical study of Pamukkale travertines: new evidences of low-temperature non-equilibrium calcite–water fractionation. Sediment Geol 238:191–212
Kele S, Breitenbach SFM, Capezzuoli E, Meckler AN, Ziegler M, Millan IM, Kluge T, Deák J, Hanselmann K, John CM, Yan H, Liu Z, Bernasconi SM (2015) Temperature dependence of oxygen- and clumped isotope fractionation in carbonates: a study of travertines and tufas in the 6–95 °C temperature range. Geochim Cosmochim Acta 168:172–192
Kim S-T, O'Neil JR (1997) Equilibrium and nonequilibrium oxygen isotope effects in synthetic carbonates. Geochim Cosmochim Acta 61:3461–3475
Laurenzi M, Stoppa F, Villa IM (1994) Eventi ignei monogenici e depositi piroclastici nel distretto ultra-alcalino Umbro-Laziale: revisione, aggiornamento e comparazione dei dati cronologici. Plinius 12:61–65
Lisiecki LE, Raymo ME (2005) A Pliocene–Pleistocene stack of 57 globally distributed benthic $\delta^{18}O$ records. Paleoceanography 20:PA1003. doi:10.1029/2004PA001071
Luthi D, Le Floch M, Bereiter B, Blunier T, Barnola JM, Siegenthaler U, Raynaud D, Jouzel J, Fischer H, Kawamura K, Stocker TF (2008) High-resolution carbon dioxide concentration record 650,000–800,000 years before present. Nature 453:379–382. ftp://ftp.ncdc.noaa.gov/pub/data/paleo/icecore/antarctica/epica_domec/edc-co2-2008.txt
Mancini M, Cavinato GP (2005) The Middle Valley of the Tiber River, central Italy: Plio-Pleistocene fluvial and coastal sedimentation, extensional tectonics and volcanism. In: Blum MD, Marriott SB, Leclair SF (eds) Fluvial sedimentology VII, vol 35. IAS Special Publication, Blackwell, Oxford, pp 373–396
Mancini M, Girotti O, Cavinato GP (2004) Il Pliocene e il Quaternario della Media Valle del Tevere (Appennino Centrale). Geol Rom 37:175–236
Mancini M, D'Anastasio E, Barbieri M, De Martini PM (2007) Geomorphological, paleontological and $^{87}Sr/^{86}Sr$ isotope analyses of Early Pleistocene paleoshorelines to define the uplift of Central Apennines (Italy). Quat Res 67:487–501
Manfra L, Masi U, Turi B (1976) La composizione isotopica dei travertini del Lazio. Geol Rom 15:127–174
Marra F, Florindo F (2014) The subsurface geology of Rome: sedimentary processes, sea-level changes and astronomical forcing. Earth Sci Rev 136:1–20
Marra F, Karner DB, Freda C, Gaeta M, Renne P (2009) Large mafic eruptions at Alban Hills Volcanic District (Central Italy): chronostratigraphy, petrography, and eruptive behaviour. J Volcanol Geotherm Res 179:217–232
Mattei M, Conticelli S, Giordano G (2010) The Tyrrhenian margin geological setting: from the Apennine orogeny to the K-rich volcanism. In: Funiciello R, Giordano G (eds) The Colli Albani volcano. IAVCEI Spec. Publ. 3, Geological Society, London, pp 7–27

Mazza R, La Vigna F (2011) Hydrogeology of the southern Middle Tiber Valley (Central Italy). AQUA Mundi 2:93–102

McCrea JM (1950) On the isotopic chemistry of carbonates and a paleotemperature scale. J Chem Phys 18:849–857

Meents WF (1960) Glacial drift gas in Illinois. Ill State Geol Surv Circ 292:1–58

Mesci BL, Gürsoy H, Tatar O (2008) The evolution of travertine masses in the Sivas area (central Turkey) and their relationships to active tectonics. Turk J Earth Sci 17:219–240

Minissale A (2004) Origin, transport and discharge of CO_2 in central Italy. Earth Sci Rev 66:89–141

Minissale A, Kerrick DM, Magro G, Murrell MT, Paladini M, Rihs S, Sturchio NC, Tassi F, Vaselli O (2002) Geochemistry of Quaternary travertines in the region north of Rome (Italy): structural, hydrologic and paleoclimatic implications. Earth Planet Sci Lett 203:709–728

Özkul M, Kele S, Gökgöz A, Shen CC, Jones B, Baykara MO, Fórizs I, Nemeth T, Chang YW, Alçiçek MC (2013) Comparison of the Quaternary travertine sites in the Denizli Extensional Basin based on their depositional and geochemical data. Sediment Geol 294:179–204

Özkul M, Gökgöz A, Kele S, Baykara MO, Shen CC, Chang YW, Kaya A, Hançer M, Aratman C, Akın T, Örü Z (2014) Sedimentological and geochemical characteristics of a fluvial travertine: a case from the eastern Mediterranean region. Sedimentology 61:291–318

Palladino DM, Simei S, Sottili G, Trigila R (2010) Integrated approach for the reconstruction of stratigraphy and geology of Quaternary volcanic terrains: an application to the Vulsini Volcanoes (central Italy). In: Groppelli G, Viereck L (eds) Stratigraphy and geology in volcanic areas, vol 464. GSA Special Papers, pp 66–84

Panichi C, Tongiorgi E (1976) Carbon isotopic composition of CO_2 from springs, fumaroles, mofettes and travertines of central and southern Italy: a preliminary prospection method of geothermal area. In: Proceedings. 2nd UN symposium on the develop and use of geothermal energy, 20–29 May 1975, San Francisco. pp 815–825

Patacca E, Sartori R, Scandone P (1990) Tyrrhenian basin and Apenninic arcs: kinematics relations since Late Tortonian times. Mem Soc Geol It 45:425–451

Pazdur A, Dobrowolski R, Durakiewicz T, Piotrowska N, Mohanti M, Das S (2002) $\delta^{13}C$ and $\delta^{18}O$ time record and palaeoclimatic implications of the Holocene calcareous tufa from south-eastern Poland and eastern India (Orissa). Geochronometria 21:97–108

Peccerillo A (2003) Plio-Quaternary magmatism in Italy. Episodes 26:222–226

Pedley HM (1990) Classification and environmental models of cool freshwater tufas. Sediment Geol 68:143–154

Pedley HM (2009) Tufas and travertines of the Mediterranean region: a testing ground for freshwater carbonate concepts and developments. Sedimentology 56:221–246

Pentecost A (1995) The Quaternary travertine deposits of Europe and Asia minor. Quat Sci Rev 14:1005–1028

Pentecost A (2005) Travertine. Springer, Berlin, p. 446

Perini G, Francalanci L, Davidson JP, Conticelli S (2004) Evolution and genesis of magmas from Vico Volcano, Central Italy: multiple differentiation pathways and variable parental magmas. J Petrol 45:139–182

Petitta M, Primavera P, Tuccimei P, Aravena R (2011) Interaction between deep and shallow groundwater systems in areas affected by Quaternary tectonics (Central Italy): a geochemical and isotope approach. Environ Earth Sci 63:11–30

Piccardi L, Monti C, Vaselli O, Tassi F, Gaki-Papanastassiou K, Papanastassiou D (2008) Scent of a myth: tectonics, geochemistry and geomythology at Delphi (Greece). J Geol Soc Lond 165:5–18

Raimondi V, Costagliola P, Ruggieri G, Benvenuti M, Boschi C, Brogi A, Capezzuoli E, Morelli G, Gasparon M, Liotta D (2015) Investigating fossil hydrothermal systems by means of fluid inclusions and stable isotopes in banded travertine: an example from Castelnuovo dell'Abate (southern Tuscany, Italy). Int J Earth Sci 105:659–679

Rodríguez-Berriguete A, Alonso-Zarza AM, Cabrera MC, Rodriguez-Gonzalez A (2012) The Azuaje travertine: an example of aragonite deposition in a recent volcanic setting, N Gran Canaria Island, Spain. Sediment Geol 277–278:61–71

Selim HH, Yanik G (2009) Development of the Cambazlı (Turgutlu/MANISA) fissure-ridge-type travertine and relationship with active tectonics, Gediz Graben, Turkey. Quat Int 199:157–163

Sibson RH (1987) Earthquake rupturing as a mineralising agent in hydrothermal systems. Geology 15:704–710

Sierralta M, Kele S, Melcher F, Hambach U, Reinders J, van Geldern R, Frechen M (2010) Uranium-series dating of travertine from Süttő: implications for reconstruction of environmental change in Hungary. Quat Int 222:178–193

Sottili G, Palladino DM, Zanon V (2004) Plinian activity during the early eruptive history of the Sabatini Volcani District, Central Italy. J Volcanol Geotherm Res 135:361–379

Sottili G, Palladino DM, Marra F, Jicha B, Karner DB, Renne P (2010) Geochronology of the most recent activity in the Sabatini Volcanic District, Roman Province, central Italy. J Volcanol Geotherm Res 196:20–30

Sturchio NC (1990) Radium isotopes, alkaline earth diagenesis, and age determination of travertine of Mammoth Hot Springs, Wyoming, USA. Appl Geochem 5:631–640

Temiz U, Gökten E, Eikenberg J (2013) Strike-slip deformation and U/Th dating of travertine deposition: Examples from North Anatolian Fault Zone, Bolu and Yeniçağ Basins, Turkey. Quat Int 312:132–140

Tremaine DM, Froelich PN, Wang Y (2011) Speleothem calcite farmed in situ: modern calibration of $\delta^{18}O$ and $\delta^{13}C$ paleoclimate proxies in a continuously-monitored natural cave system. Geochim Cosmochim Acta 75:4929–4950

Tuccimei P, Conforti M, Funiciello R, Soligo M (2001) Datazioni U/Th delle placche travertinose di Fiano Romano e Pian Paradiso (Lazio, Italia), FIST GeoItalia 2001 Symposium Abstract, pp 124–125

Turi B (1986) Stable isotopes geochemistry of travertines. In: Fritz P, Fontes JC (eds) The terrestrial environment. Handbook of environmental isotope geochemistry, vol 2B. Elsevier, Amsterdam, pp 207–238

Uysal T, Feng Y, Zhao J, Altunel E, Weatherley D, Karabacak V, Cengiz O, Golding SD, Lawrence MG, Collerson KD (2007) U-series dating and geochemical tracing of late Quaternary travertines in co-seismic fissures. Earth Planet Sci Lett 257:450–462

Van Noten K, Claes H, Soete J, Foubert A, Özkul M, Swennen R (2013) Fracture networks and strike-slip deformation along reactivated normal faults in Quaternary travertine deposits, Denizli Basin, western Turkey. Tectonophysics 588:154–170

Vaselli O, Tassi F, Minissale A, Capaccioni B, Magro G, Evans WC (1997) Geochemistry of natural gas manifestations from the Upper Tiber Valley (Central Italy). Mineral Petrogr Acta 40:201–212

Ventriglia U (2002) Geologia del territorio del Comune di Roma. Provincia di Roma, Rome, p 810

Vignaroli G, Berardi G, Billi A, Kele S, Rossetti F, Soligo M, Bernasconi SM (2016) Tectonics, hydrothermalism, and paleoclimate recorded by Quaternary travertines and their spatio-temporal distribution in the Albegna basin, central Italy: insights on Tyrrhenian margin neotectonics. Lithosphere 8:335–358